(1)

AR
U3

UTAH RESEARCH & DEVELOPMENT CO., INC.
SALT LAKE CITY, UTAH
Subsidiary of Interstate Engineering Corporation, Anaheim, California

SPONSORED BY:
Advanced Research Projects Agency
U. S. Army Natick Laboratories
Natick, Massachusetts
ARPA Order No. 267 Amendment No. 4

FINAL REPORT
PHASES I and II

THEORETICAL AND EXPERIMENTAL STUDY OF LOW-VELOCITY PENETRATION PHENOMENA

Contract No. DA 19-129-AMC-150(X) (OI 9114)

28 JUN 1964

Utah Research & Development Co.
2175 South 3270 West
Salt Lake City, Utah

Phone: 486-1301
TWX: 801-521-2680

TABLE OF CONTENTS

TABLE OF CONTENTS (Continued)

TABLE OF CONTENTS (Continued)

ABSTRACT

This report is a technical summary of Phases I and II of a theoretical and experimental study of low-velocity penetration phenomena.

Phase I has consisted of a literature survey to determine the state of the art. The results are summarized and a bibliography is included. It is concluded that semi-empirical correlation formulae and over-simplified theories do not give the results needed for armor design and are inadequate as a guide to understanding low-velocity impact phenomena.

Phase II has consisted of the development of a new method of describing the elasto-plastic behavior of a material under impact conditions. The non-linear differential equations involved are expressed in a tensor formulation particularly suitable for computer calculations. The method used is very general and allows a wide variety of boundary conditions and material properties to be used. The work is described and the results of preliminary calculations are presented in this report.

I. INTRODUCTION

Phase I has consisted of a literature survey to determine the present state of knowledge in the field of low-velocity impact. The literature was searched to determine the information available on the absorption of energy by the target during impact, the mechanisms involved in impact, theories of impact in armor penetration and comparison of data with theory. The purpose was to determine the present state of knowledge and to find a basis for the development of further theory. This report contains a brief summary of the results of the literature survey, a bibliography of pertinent literature, and a discussion of the possible courses for further work with the reasons for choosing the particular course indicated in Phase II.

Phase II has consisted of the development of a detailed theory of impact. This report includes a description of a new mathematical method which has been developed for solving the equation involved in low-velocity impact in a visco-elastic material. At the present time this theoretical formulation and computer solution of the impact problem appear to have great promise. The techniques are general and have application to a wide range of materials and to a variety of impact conditions. Preliminary computations show agreement with other work and indicate that the extension can be made to problems of armor development.

An oral report of progress under Phase II of this contract was given at the Armor Conference held in Natick, Massachusetts, May 19 and 20, 1964. The part of this report covering Phase II of the work is also being submitted as a report on that conference.

II. PHASE I - RESULTS OF LITERATURE SURVEY

1. CLASSIFICATION OF PAST WORK

Past experimental and theoretical work on armor penetration and impact phenomena may be classified arbitrarily under the following four headings:

1. Exploratory Research
2. Phenomenological Models
3. Correlation Laws
4. Detailed Theory.

Much of the experimental work can be classified as exploratory. Materials of interest have been used as targets and impacted with several types of projectiles traveling at various velocities. The materials used have included metals, ceramics, organic materials, and composite materials. Targets have been single thin plates, multiple plates, semi-infinite targets and complex structures of various types. Data obtained have been target damage and the velocity and size of material leaving the back and front sides of the target. From this work a large body of data has been obtained which gives a guide to expected results in any limited area. Within a narrow range of materials and conditions, the expected results can be predicted simply on the basis of limited extrapolations of existing data.

The data from this exploratory work led naturally to the next step, that of developing phenomenological models of the processes occurring. Many types of simple models have been developed. Most of them have come about as a result of assuming that a certain process was predominant in producing the effect observed and then writing simplified equations describing this process and adjusting parameters to fit the data. This work has resulted in the development of successful correlation laws which can be used when conditions do not depart far from those assumed in the model. This approach has proved to be very unsuitable in the case of complex situations. None of the models are general enough to actually describe any complex situation, so fail to give any insight into expected results as parameters are varied. They fail particularly when the geometry is complicated, as with composite targets or when the material is little understood as is the case with brittle materials or where the basic phenomena change, such as from hydrodynamic to elastic.

In an attempt to obtain results of more general validity, various correlation laws have been developed usually based on dimensional analysis. The aim has been to take all data and fit it into a unified relationship. These various correlation laws have proven to be useful in the high-velocity impact

phenomena in simple targets, but have proven to be unreliable for complicated geometries or materials or for data beyond the range where the law was developed.

To correct the faults of all these semi-empirical approaches, attempts have been made to obtain a complete description of the impact process; that is, to develop a theory which describes in detail the time-history of the material displacement. Because of the complexity and difficulty of this problem, these theoretical developments have so far been limited to rather simple cases which do not match the actual impact situations involved and are not general enough to apply to new conditions.

2. CURRENT RESEARCH

Current research is extensive in all of the areas indicated above. Exploratory work is being done in the areas where data are almost completely lacking from past work, particularly in the use of brittle materials such as ceramics, glasses, and brittle metals; in the use of structures with complex geometry and in the use of various combinations of materials. This work is not general but specific cases are being examined independently. No theoretical framework exists to guide the direction of the experimental work. In the low-velocity impact range, any ingenious idea which can be developed can be quite easily tested, but the exploratory work in this area gives little hope of coming up with any new ideas based solely on the results from past tests since there is no general understanding of the phenomena involved to lead to decisions as to how to make better materials.

In the area of developing new phenomenological models and better correlation laws, some progress is being made. Considerable work is being done on measuring various factors which are important in impact and cratering and penetration and basing the models and correlation laws on these measured results. Instead of simply looking at the amount of damage done or the residual velocity after penetration, measurements are being made of the actual energy absorbed into the material, the momentum transferred, or the strength of waves. Quantities which relate to details of the phenomena occurring are being observed and measured. The hope is that better correlation laws and better understanding necessary for inventive armor design will be obtained. This work is presently limited to very simple situations, usually to simple ductile materials and to semi-infinite targets. This work has not been extended at all to the complex materials which seem to be most promising for armor for low-velocity impact protection. This empirical work is not leading directly to a general understanding of the problems involved or developing a general theoretical framework for advancing the state of the art; however, it is producing important data which must be used for testing

and guiding any theory, and which is certainly the only present guide to armor development.

Considerable work is now being done on extending the theory. As in the past, work is being done on developing simplified theories which can be solved analytically and in developing simplified theories which can only be solved by numerical techniques with computers. The original solution of two-dimensional impact problems by Bjork, Harlow and others has been extended and modified in attempts to give results which are more complete and satisfactory. Techniques are being developed and tested for adding viscosity or elasticity to the formulation of the material properties as used in the original hydrodynamic formulation of the problem. These extensions are applicable in high-velocity impact but are not satisfactory in the low-velocity impact region where the process is not hydrodynamic but where elasticity and strength of materials predominate and where plastic flow is more important than inviscid flow.

3. CONCLUSIONS AND RECOMMENDATIONS

This literature survey has indicated that no past work nor present research is adequate to solve the problem of low-velocity impact phenomena in the general manner which is desired. Surely experimental determination of the effects obtained using different armor materials will continue to bring results and will provide the ultimate test for any material; however, experiment and intuition are an inadequate guide in complex situations without some insight based on a theoretical understanding of the phenomena involved. We conclude that the greatest need at present is for a theory which describes the observed phenomena in detail.

The approach of attempting to modify the hydrodynamic theory previously used in high-velocity impact is the wrong approach to use when the basic phenomena are different. For this reason, we have decided that a theoretical approach beginning from elasto-plastic deformation theory is the proper approach to use since these phenomena predominate under the conditions met in low-velocity impact. This approach is also of significance for high-velocity impact theory since strength and viscosity predominate in the later stages of high-velocity impact and are probably controlling in the determination of the end results obtained. The material properties developed from high-velocity impact studies, again, are not applicable to the problem here. Material properties are only partly understood in the elasto-plastic regime and any theoretical work must be based on experimental and theoretical understanding of material properties.

The theoretical approach which we have undertaken is discussed separately in Section IV below. It is based on a new formulation of the stress-strain laws and equations of motion suitable for computer solution. The method is very general and is applicable to any material for which the material properties can be determined and to a wide variety of target geometries. Preliminary results are presented and show that the method has promise. The direction for future research is indicated.

III. LITERATURE REVIEW

The bibliography is divided into two parts. Part 1 contains a list of compiled bibliographies and proceedings of symposiums and seminars concerning impact and body armor. Part 2 contains a list of pertinent books and papers.

Many of the articles listed in Part 2 are summarized. These articles have also been evaluated to some extent as to content by use of the symbols listed below.

Symbol	Description
M	Metal Targets
NM	Non-metal Targets
HV	Velocities Above 10,000 feet per second
LV	Velocities Below 10,000 feet per second
Th	Theoretical Program
Ex	Experimental Program
Thk	Thick (semi-infinite) Targets
Thn	Thin Targets (plates, etc.)
E	Concerns Energy Partitioning or Dissipation

1. PART 1 - SYMPOSIUMS, BIBLIOGRAPHIES AND SEMINARS

Graham, R., "Bibliography on Impact Physics"
Sandia Corporation
Bibliography, SCR-59 December 1958

This bibliography consists of a rather complete collection of references and abstracts on the subjects of:
(1) Plastic Wave Propagation in Bounded Solids
(2) Behavior of Metals Under Explosive Conditions
(3) Dynamic Photoelasticity
(4) Penetration Phenomena.
Other topics covered in less detail are:
(5) Behavior of Materials at High Strain Rates
(6) Lateral Impact
(7) Impact Measurement Devices.

General references at the beginning of the bibliography cite articles or books which cover the field of impact. An author index and a chronological listing of articles within a particular topic are included.

Proceedings of the First Hypervelocity Impact Symposium
RAND Corporation
Santa Monica, California 1955

Proceedings of the Second Hypervelocity Impact Symposium
U. S. Naval Research Laboratory
Washington, D.C. 1957
Two volumes
W. C. Mannix, W. W. Atkins and R. E. Clark, Editors

Proceedings of the Third Hypervelocity Impact Symposium
Armour Research Foundation of Illinois Institute of Technology
Chicago, Illinois 1959
Two volumes
F. Genovese, Editor

Proceedings of the Fourth Hypervelocity Impact Symposium
Air Proving Ground Center
Air Research and Development Command
United States Air Force
Eglin Air Force Base, Florida 1960
Three volumes and one supplement

Proceedings of the Fifth Symposium on Hypervelocity Impact
Colorado School of Mines
Denver, Colorado 1962
Two volumes

Proceedings of the Sixth Symposium on Hypervelocity Impact
The Firestone Tire and Rubber Company
Cleveland, Ohio 1963
Four volumes

Rogers, Marguerite M., "Bibliography of Papers of Interest to Body Armor"
in Applied Mechanics Review through December, 1955
University of South Carolina 1956

A literature search has been made through all issues of the Applied Mechanics Review for references which may be pertinent to the subject of penetration of projectiles into plastic-elastic substance. The references are given in order of the abstract number and year as given in Applied Mechanics Review.

Seminar on HEP Shell
Stanford Research Institute
Stanford, California February 1955

Seminar where the following papers were presented:

1. "Mechanism of Spalling," Eugene F. Poncelet
2. "Experimental Studies of Shock Pulses in Steel," Samuel Katz
3. "Hydrodynamic Theory of Shock in Steel," George E. Duvall
4. "Factors Affecting Detonation Rate and Pressure and Shape of Detonation Front," Thomas C. Poulter

Symposium on Personnel Armor
U. S. Naval Research Laboratory
Washington, D.C. 4-5 October 1961

1. "Characterization of Textile Yarns for Use Under Ballistic Impact Conditions," Jack C. Smith
2. "Dynamic Behavior of Textile Fibers and Structures as Related to Personnel Armor," Henry M. Morgan
3. "A Theoretical Study of Penetration and Residual Projectile Velocities," L. E. Fugelso
4. "Method for Obtaining Yield Stresses at High Strain Rates," J. W. Corcoran
5. "The Dynamic Properties of High Tenacity Yarns and Their Relationship to Ballistic Resistance," R. C. Laible
6. "Buoyant Insulating Body Armors from Staple Fibers," M. C. Jaskowski
7. "Some U. S. Army Research Office Sponsored Research," Sherwood Githens, Jr.
8. "Development of QMC Composite Armor Vest," E. R. Barron
9. "The Effect of Resin Concentration on Physical Properties of a Laminated Structure for a Crash and Ballistic Protective Flight Helmet," Abraham L. Lastnik and John W. Gates
10. "A Set of Angles of Obliquity for Use in Assessing Body Armor," Herbert Maisel, Wallace Chandler and Gerald DeCarlo.

2. PART 2 - BOOKS AND PAPERS

Abbott, K. H., "Metallurgical Observations of High Speed Impact,"
4th Symposium of Hypervelocity Impact, Vol. II, AFGC-TR-60-39
September 1960

M, LV, Ex

Cylindrical pellets, 0.4 inches in diameter and 0.50 inches long, machined from annealed 1020 steel and from fully hardened

FS x 318 steel, were fired at 1.50 inch thick rolled homogeneous armor plates. The velocity range covered was from 2000 ft/sec to approximately 10,000 ft/sec. The crater parameters were measured for each impact, and the plate material adjacent to the crater was examined metallurgically. The effects on crater formation and the resulting metallurgical aspects of crater formation are evaluated.

Allen, W. A., Mapes, J. M., and Mayfield, E. B., "Shock Waves in Air Produced by Waves in a Plate," J. Appl. Phys. 26, 1173, 1955

M, Ex
Contains photos showing that the bulge on the rear face of a steel plate has limbs that are almost straight.

Allen, W. A. and Rogers, J. W., "Linearized Theory of the Penetration of a Rod into a Thick Target,"
U. S. Naval Ordnance Test Station
China Lake, California
NAVWEPS Report 7906, Copy 290 April 1962

Th
A linearized theory is proposed for the penetration of a rod into a thick target. Hydrodynamic theory, based upon a constant dynamic yield strength of the target, yield a relationship involving penetration velocity and the density ratio of the target with respect to the rod. The proposed theory, for the case of six rod materials and an aluminum target, represents the experimental data better than the conventional hydrodynamic theory based upon a constant dynamic yield strength of the target.

Atkins, W. S., "Flash Associated with High-Velocity Impact on Aluminum," J. Appl. Physics 26, 176, 1955

Ex
Shows photos of straight-limbed bulge on rear face of an aluminum plate.

Backman, M. E., "Elastic and Plastic Behavior in the Impact of Cylinders Against Plate," J. Appl. Physics 30, 1397, 1959

M, Th, Ex, Thk
A theory of the indentation of a thick plate from impact by a flat-ended elastic cylinder is derived from elastic and plastic theories and compared to experimental values for 2024-T4 aluminum alloy, half-hard naval brass and Armco iron. Plastic conditions in plates

of the aluminum alloy are considered in detail by assuming increase in hardness to a maximum value. These results are sensitive to projectile length and are compared to experimental results for five projectile lengths.

Barron, E. R., "Development of QMC Composite Armor Vest,"
Quartermaster Research and Engineering Command
U. S. Army
Natick, Massachusetts October 1961

Descriptions are given for types of body armor that have been used previously through the ages. The details of a Doron vest used in the Korean War are given, along with reasons for discarding same. Present vest is built up of composite armor of ballistic nylon and .032 titanium (4 plys). No information is given pertaining to the efficiency of this newest vest.

H. W. Kuhlmann, R. I. Leininger, R. G. Heiligmann and E. E. McSweeney "Development of Laminated Armor,"
Battelle Memorial Institute April 28, 1949

Final report under Contract W-33-019-Ord-6266.

Bell, J. F., "Propagation of Plastic Waves in Solids," J. Appl. Physics, Vol. 30, No. 2, Feb 1959

Ex, M, LV
A detailed experimental study of large amplitude plastic waves in annealed aluminum is presented. Using the author's diffraction grating technique, accurate strain-time and surface angle-time histories are obtained at different locations in the velocity of impact. Verification of the strain rate independent theory with strain amplitude modification is provided in this region for impact velocities up to 63 ft/sec. Poisson's ratio is dynamically determined for strains up to 0.5%. Marked changes are observed in the propagation behavior above 1.06% strain, related to the abrupt increase in Poisson's ratio from 1/3. The maximum amplitude of waves above this value decreases exponentially with distance from impact.

Beth, R. A., "Penetration Theory: Separable Force Laws and the Time of Penetration,"
Princeton University OSRD, 5258, ATI 24842 June 1945

Th
The separable force laws represented by $R=C.g(X)\cdot f(v)$ are summarized. For a separable force law the relationship between x

and v during penetration can be expressed in terms of the striking velocity v_o, and the maximum penetration x_1 in such a way that the mass of the projectile and the target strength parameter C are eliminated. This leads to a simplified formula for computing the times of penetration.

Bethe, H. A., "An Attempt of a Theory of Armor Penetration,"
Cornell University
Ordnance Laboratory
Frankford Arsenal
May 1941

Ex, M, NM

Early endeavor to describe by simple mathematical models the mechanism of armor penetration. Fairly good qualitative information describing resistive ability of armor and plastic work.

Beye, W. R., Sacks, I., Mahan, F. T., Jr., Barker, F. J., "Design Manual for Personnel Armor,"
Watertown Arsenal Laboratory
Watertown, Massachusetts
February 1951

Ex

The numerous factors involved in the general problem of designing body armor to provide maximum resistance to penetration of munition fragments have been investigated by the Midwest Research Institute under contract to the Ordnance Corps. The results of this work, together with those of other agencies have been summarized and brought together in the form of a manual for use in designing body armor. Since a knowledge of the probable striking velocity, weight, size and other characteristics of fragments is an important prerequisite to the design of body armor and to an estimation of its ability to prevent or reduce casualties, all available data on fragment characteristics have been included in this manual. In addition to the data, mathematical procedures are developed for handling the numerous variables and reducing the data to a form easily applied to problems of body armor design. Examples are given to illustrate the design methods and some comparisons are given to show the relative performance of some of the current leading body armor materials under conditions of fragment impact expected in combat.

Beye, W. R. and Witherspoon, J. F., "Study of the Behavior of Light Personnel Armor Consisting of Metallic, or a Combination of Fibrous and Metallic Materials,"
Watertown Arsenal
Watertown, Massachusetts

Ex, M, NM, LV, Thn

During a previous work a method was developed to describe the resistance to penetration by fragments having various masses and velocity. This report presented data for 1/2" diameter cylinders projected perpendicularly against the armor materials. The present work considers projectiles impacting at various angles of incidence, different projectile nose shapes, different fragment sizes and higher velocities.

Biot, M. A., "Theory of Deformation of a Porous Viscoelastic Anisotropic Solid," J. Appl. Physics, Vol. 27, No. 5, Page 489, May 1956

Th

Equations are established for the deformation of a viscoelastic porous solid containing a viscous fluid under the most general assumptions of anisotropy. The particular cases of transverse and complete isotropy are discussed. General solutions are also developed for the equations in the isotropic case. As an example, the problem of the settlement of a loaded column is treated. The second order effect of the change of permeability with deformation is also discussed.

Biot, M. A., "Mechanics of Deformation and Acoustic Propagation in Porous Media," Journal of Applied Physics, Vol. 33, No. 4, April 1962

Th

A unified treatment of the mechanics of deformation and acoustic propagation in porous media is presented, and some new results and generalizations are derived. The writer's earlier theory of deformation of porous media derived from general principles of non-equilibrium thermodynamics is applied. The fluid-solid medium is treated as a complex physical-chemical system with resultant relaxation and viscoelastic properties of a very general nature. Specific relaxation models are discussed, and the general applicability of a correspondence principle is further emphasized. The theory of acoustic propagation is extended to include anisotropic media, solid dissipation, and other relaxation effects. Some typical examples of sources of dissipation other than fluid viscosity are considered.

Bjorksten Research Laboratories, Inc., "Investigation and Development of Body Armor Structures,"

Final report under Contract DA-19-129-QM-596.

Bluhm, I. I., "Stresses in Projectiles During Penetration," Proc. SESA, 13, 167, 1956 1956

Thin plates were fired at stationary projectile.

Bridgman, P. W., "Effects of High Hydrostatic Pressure on the Plastic Properties of Metals," Review of Modern Physics, Vol. 17, p. 3, 1945

BRL Report No. R-902, "Mechanisms of Armor Penetration," February 1951

CLASSIFIED

Bruce, E. P., "Review and Analysis of High Velocity Impact Data," 5th Symposium on Hypervelocity Impact Volume 1, Part 2 October 1961

Ex, M, Thk, LV, HV

A thorough review has been made of existing experimental data applicable to the impact of high velocity projectiles with semi-infinite metal targets. Empirical equations relating depth of penetration and crater volume to properties of the projectile and target have been derived based on the assumptions that:

1. Projectile shape does not affect crater shape for projectiles which range from spheres to cylinders up to one caliber in length, and
2. Craters are hemispherical.

Both of these assumptions are supported by the available data. Additional data and/or a rigorous theoretical treatment of the problem are required to evaluate the utility of the equations at higher impact velocities.

Charters, A.C., "High Speed Impact," Scientific American, Vol. 203, p. 128, No. 4. October 1960

A summary of the phenomena of impact written for the layman. There is a brief history of the work done and who is doing the investigations (at the time the article was written). Many photographs of various types of impact are included.

Chou, Pei Chi, "Visco-Plastic Flow Theory in Hypervelocity Perforation of Plates," 5th Symposium on Hypervelocity Impact, Vol. I, Part I, Nonr-(G)-0020-62(X), October 1961

Th, Thn

In the analysis of the hypervelocity impact problem, only two theories have been used: the incompressible hydrodynamic theory and the compressible shock wave theory. Both of these theories consider the solid materials under impact as fluids, and the analyses are similar to that for standard perfect fluid theory in fluid mechanics, where the viscosity of the fluid is neglected. For certain special cases of impact, the omission of viscosity may be justified, but the fact is that an exact understanding of the effect of the viscosity is still unknown.

In order to gain some insight into the effect of viscosity, the case of the perforation of a thin plate by a circular cylinder is considered. Based on available test results, it is felt that viscosity plays a more important role in perforation problems than it does in cratering problems. Visco-plastic properties of the material are assumed and the governing equations derived. The solution of these equations are plotted in the form of velocity displacement, strain and strain-rate vs radial distance curves. The perforation diameter, loss of momentum and residual velocity of the projectile are also obtained.

Clark, D. S. and Wood, D. S., "The Time Delay for the Initiation of Plastic Deformation at Rapidly Applied Constant Stress," Proceedings, American Society for Testing Materials, Vol. 49, p. 717 1949

Clark, D. S. and Wood, D. S., "The Tensile Impact Properties of Some Metals and Alloys," Transactions, American Society for Metals, Vol. 42, p. 45 1950

Collins, Rufus D. and Kinard, William H., "The Dependency of Penetration on the Momentum Per Unit Area of the Impacting Projectile and the Resistance of Materials to Penetration,"
National Aeronautics and Space Administration
Technical Note D-238 May 1960

Ex, Thn, M

The results of this investigation indicate that the penetration of projectiles into quasi-infinite targets can be correlated as a function of the maximum momentum per unit area possessed by the projectiles. The penetration of projectiles into aluminum, copper, and steel targets was a nonlinear function of the momentum per unit area of the impacting projectiles. Penetration varied inversely as the projectile density and the elastic modulus of the target material for a given projectile momentum per unit area.

Crater volumes were found to be a linear function of the kinetic energy of the projectile, the greater volumes being obtained in the target materials which had the lowest yield strength and the lowest speed of sound.

Corcoran, J. W. and Kelly, J. M., "Further Studies in the Behavior of Lightweight Personnel Armor Materials,"
Quartermaster Research and Engineering Command November 1962

Ex, M, LV, Thn

A series of tests was carried out to provide information on the behavior of projectiles impacting two types of armor materials at oblique and normal incidence in the velocity range 1000 ft/sec to 4000 ft/sec. The armor materials were a titanium alloy and a high-test steel and the projectiles used were high tensile strength cylinders. The report includes the results of tests to determine the yield characteristics of the armor at high strain rates.

Corcoran, J. W., Kelly, J. M., "Phenomena of Penetration in Light Weight Personnel Armor Materials,"
Quartermaster Research and Engineering Command
Beckman & Whitley, Inc. November 1962

A program of test work was undertaken to provide data on the behavior of projectiles impacting light armor materials, at velocities in the range 1000 ft/sec to 4000 ft/sec. The report includes the results of tests of spherical and cylindrical aluminum projectiles impacting aluminum plates and similar projectiles impacting a light armor built up out of corrugated aluminum sheets. It concludes with a description of a new method for determining material properties at high speed rates. This method was used to obtain estimates of the yield stress of 2024 T4 aluminum at strain rates from 2900/sec to 13,600/sec.

Curran, Donald R., "Nonhydrodynamic Attenuation of Shock Waves in Aluminum,"
J. Appl. Physics, Vol. 34, No. 9 September 1963

Ex, M, Thn

The attenuation of shock waves in 2024 aluminum has been studied experimentally by impacting aluminum flyer plates upon aluminum targets and measuring the target-free surface velocity as a function of target thickness. The results disagree with the predictions of hydrodynamic theory, exhibiting premature attenuation. An elastic-plastic model is proposed which adequately describes the data. In this model, Poisson's ratio remains constant under compression and

the tensile yield strength increases linearly with compression, attaining a value of 12 kbars at a relative volume V/V_o of 0.86.

Davids, N., Huang, Y. K. and Jaunzemis, "Some Theoretical Models of Hypervelocity Impact."
5th Symposium on Hypervelocity Impact
Vol. I, Part I, Nonr-(G)-0020-62(X) October 1961

Th
The phenomena of cratering is complex because different effects predominate in different parts of the crater. Thus in a zone ahead of the projectile, the target material is under ultra-compression. This zone is bounded in front by an advancing shock wave and gradually shades off at the sides into another zone where the material, in some state of fluidity, deforms sideways along the crater. Ultimately, as the angle of deviation from the direction of impact is increased, the material has undergone permanent plastic deformation and hills up to form the lip of the crater.

The direct aim of any penetration theory is, of course, to predict the shape and size of the crater. The spherical model does this by analyzing the state of the material in the region behind the shock wave, and leads to a value for the diameter and volume of the crater comparable with experimental data.

Dieter, G. E., Jr., "Mechanical Metallurgy,"
McGraw-Hill Book Company
New York, New York 1961

Chapters 3 through 8 give basic introduction to the plastic behavior of metals.
Chapter 3 - Elements of Theory of Plasticity
Chapter 4 - Plastic Deformation of Single Crystals
Chapter 5 - Plastic Deformation of Polycrystalline Aggregates
Chapter 6 - Dislocation Theory
Chapter 7 - Fracture
Chapter 8 - Internal Friction

Encyclopedia Brittanica, "Armour Plate, Resistance to Penetration,"
1959 Edition

French, A. P., "Dissipation of Projectile Energy on Impact,"
University of South Carolina
Technical Note No. 11-57-P1 1957

Ex, M, NM, Thn, LV, E

The research has been concerned primarily with the details of energy loss for projectiles entering materials of interest as defensive armor. Much of the work has been done on nylon fabric -- its mechanical properties and its ability to absorb energy from non-deforming projectiles. A considerable amount of work has also been done on certain other materials in the form of solid sheets or plates. The object has been to develop theoretical considerations and to obtain new data on energy dissipation, with a view to understanding the mechanisms, and so paving the way towards improved design possibilities.

Work has been done using .15, .22, .30, .45 and .50 caliber fragment simulators. The targets used are unbonded nylon, doron (plasticized fiberglass) 24 ST aluminum, 75 ST aluminum, and Hadfield steel. General equations to include caliber are given.

French, A. P., "Penetration of Ballistic Projectiles,"
University of South Carolina
Technical Note No. 10-57-P3

Ex, NM, LV

The research has been concerned primarily with the penetration of non-deforming projectiles into aggregates of brittle particles of a well defined character. Specifically, the major part of the work has been done with spherical glass beads of various sizes. The object has been to obtain precise information on the penetration as a function of the projectile velocity, target particle size, and other relevant parameters; and to build a quantitative theory of ballistic penetration in the light of the experimental data. It is felt that this aim has been substantially achieved.

Fowles, G. R., "Attenuation of the Shock Wave Produced in a Solid by a Flying Plate," J. Appl. Physics, Vol. 31, No. 4, p. 655, April 1960

Th, M

The attenuation of the plane shock wave produced in a solid by a flying plate of the same material is treated, neglecting dissipative processes and effects of material rigidity. Explicit formulae for the position of the shock front and the shape of the pulse as functions of time are obtained by

application of Friedrich's method. A numerical example for an aluminum target and projectile is presented to illustrate some of the features of the calculation, and an experiment is proposed to test the theory. The experiment should also allow a reasonably precise measurement of sound velocity immediately behind the shock front to be obtained. This possibility applies equally well to the case of target and projectile of different materials.

Fuchs, O. P., "Impact Phenomena," AIAA Journal September 1963

Th, Ex

A statistical interpretation of experimental results derived from a small number of test shots strongly indicated that the motion of penetrating bodies might be governed by the combined result of at least three different kinds of laws of resistance acting simultaneously upon the moving body. Considering the fact that during the penetration the relative velocity between the target and projectile varies from a maximum speed to zero, the three laws of resistance have been chosen as functions of the zero, first and second powers of instantaneous velocity. As a result, a differential equation has been adopted as a working hypothesis. Finally, suitably chosen integrations lead to equations that describe penetration depth and penetration time as a function of the instantaneous velocity. A comparison between theoretically predicted results and experimental results is shown.

Fugelso, L. E., "A Theoretical Study of Dynamic Plastic Deformation Under Impact Loads,"
5th Symposium on Hypervelocity Impact
Vol. I, Part I, Nonr - (G) -0020-62 (X) October 1061

Th, Thk

A theoretical treatment of dynamic plastic deformation under impulsive loads is presented. Equations of motion based on dislocation theory are employed. The specific problem solved is the deformation of a semi-infinite half space which is struck suddenly by a cylindrical projectile. The method of solution is based on a set of continuous equations derived from discrete-dislocation theory of plastic deformation. The basic physical assumption of this model of deformation is that the total deformation of the medium is composed of elastic deformation or distortion of the body accompanied by the motion of dislocations under the applied stress.

Fugelso, L. E., Arentz, A. A., Jr., Poczatek, I. I., "Mechanics of Penetration," Vol. I, "Metallic Plates, Theory and Applications" 1961

The elastic and dynamic plastic equations of motion for the stresses and displacements in a metallic plate under impact of a metallic cylindrical punch are analytically and numerically solved. An elementary theory for time to fracture under high, rapid stresses is developed. Several engineering applications arising in thin plate penetration are solved utilizing the theory.

Fyfe, I. M., "Application of 'Hydrodynamic' Theory to the Low Stress Range of Hypervelocity Impact Problems,"
5th Symposium on Hypervelocity Impact
Vol. I, Part I, Nonr - (G)-0020-62(X) October 1961

Th
An essential feature of a mathematical model for a physical phenomenon is that it be tractable to known methods of solution. In stress wave propagation this is often achieved by making certain simplifying assumptions, as for example, when the material behaves elastically, or for higher stresses when it follows a particular elasto-plastic rule of behavior (yield criteria). It is the purpose of this paper to show that by limiting the physical configurations of the phenomenon it is possible to reduce the mathematical complexity of a mathematical model without imposing any undue restriction on the physical properties of the material under consideration.

Though the particular theory developed is not restricted to any stress level, it is regarded as being mainly applicable to low stress levels where the assumption that the medium is a fluid may not possibly be valid. In hypervelocity impact, low stresses will occur near the rear surface of a plate when a wave reflects from that surface, or in the tail of a stress pulse.

Gehring, J. William, Jr., "Observations of the Phenomena of Hypervelocity Impact,"
4th Symposium of Hypervelocity Impact
APGC-TR-60-39, Vol. II, September 1960

Th
A critical examination is made of the step-by-step mechanism of crater formation under condition of hypervelocity impact. The formation of a crater is treated as a three-step process, encompassing the primary penetration of the impacting pellet, the

descriptive analysis of the stress field causing cavitation within the material, and lastly, the elastic and/or plastic recovery of the walls of the crater. A model of crater formation is developed based upon both available theory and experimental techniques which permit the monitoring of the complete process.

Giere, A. C., "Calculating Fragment Penetration and Velocity Data for Use in Vulnerability Studies,"
U. S. Naval Nuclear Ordnance Evaluation Unit
Albuquerque, New Mexico October 1959

Th, Ex, Thn, M, LV

A brief summary of the theoretical and semiempirical penetration formulae is given. Two semiempirical expressions are employed for predicting the penetration of a strong ductile steel, one for fragment velocities less than 3,000 ft/sec, the other for velocities between 3,000 and 6,000 ft/sec. For mild-steel and aluminum-alloy armor, use is made of empirically derived formulae from the work at The Johns Hopkins University, Project Thor. The formula of R. W. Gurney is used for predicting the initial velocities of fragments from exploding shells and the actual striking velocities are calculated by considering air drag. Several approximate methods are suggested for predicting residual velocities of fragments which perforate target material. The information presented should serve only as a guide in predicting actual results in regard to vulnerability of weapons to fragments.

Ginns, D. W., "The Mechanical Properties of Some Metals and Alloys Broken at Ultra High Speeds," Journal, Institute of Metals, Vol. 61, p. 61
1937

Glass, C. M. and Pond, R. B., "A Metallurgical Approach to the Hypervelocity Problem,"
4th Symposium on Hypervelocity Impact
APGC-TR-60-39, Vol. III September 1960

Th, M, Thk

The influence of physical properties, such as modulus, ductility, fracture stress, etc., on metal deformation at high velocity is often ignored, and hydrodynamic conditions are assumed to hold true during the deformation. This approach introduces large sources of error in many cases. Under hypervelocity impact conditions of a fragment striking a semi-infinite target, the physical properties of the target are the determining factors in the target reaction. The crater produced, and total stressed region in the target, are described in terms of stress-strain relations in the

target material. This approach predicts a linear variation of crater volume and stressed region volume, with the energy of the incoming fragment.

Goldsmith, W., "Impact"
Edward Arnold, London 1960

Graham, R. A., "Depth of Indentation on an Impacting Projectile,"
J. Appl. Physics, 31:619-20, March 1960

Ex, NM
Experiment in which a 1018 steel projectile is fixed at high velocity and impacted upon a barium titanate ceramic to study the ferroelectric charge release from the barium titanate.

It was noted the flat faced projectile was indented by the flat face of the target and the depth of indentation was a function of impact velocity.

Halperson, S. M. and Atkins, W. W., "Observation of Hypervelocity Impact,"
5th Symposium on Hypervelocity Impact
Vol. I, Part 2, October 1961

Ex, M, HV, Thk
Particular attention has been given to impact studies of both hard and soft aluminum, 2014 and 1100 F, and two types of steel, 1020 and hardened 4340 steel. Spheres of aluminum and nylon (3/8" diameter) were the principal penetrators for these studies. The highest velocities were 6.03 km/sec with an aluminum sphere and 5.64 km/sec with a nylon sphere. Aluminum spheres of 1/4" diameter were also fired; maximum velocity was 6.27 km/sec.

Although much new information has been obtained about hypervelocity impact phenomena, still more data at higher velocities are needed before several pertinent questions can be answered. The effect of target strength is not yet resolved, although it appears from the E/V values for the different grades of aluminum and steel that at the velocities attained, physical properties are important.

Hauser, F. E., Simmons, J. A. and Dorn, J. E., "Strain Rate Effects in Plastic Wave Propagation,"
Metallurgical Society Conference, Estes Park Colorado, July 1960
Proceedings of Response of Metals to High Velocity Deformation Conference, Interscience Publishers, Page 93, Vol. 9

Th

Presentation of a method by which the plastic properties of materials can be investigated at strain rates up to 1.5×10^4/sec through impulsive loading techniques. Comparison is made between the elasto-plastic and strain rate theories showing that elasto-plastic theory cannot account for plastic behavior for the range of strain rates obtained and that the customary Molvern strain rate theory fails to properly take account of structure in determining strain rate effects. A description is given of strain rate effects in terms of dislocation theory and the existence of a limiting strain rate is deduced from dislocation processes.

Herrmann, W. and Jones, A. H., "Survey of Hypervelocity Impact Information,"
Massachusetts Institute of Technology September 1961

Ex, M, Thk, Thn, LV, HV

Available information relating to cratering and penetration in metallic targets has been gathered. Impact of compact particles, micro-particles, and rods at normal and oblique targets and on thin targets, multiple spaced targets, and shielded targets is considered. Experimental data is presented in tabular and graphical form for ready references. Available theories and semiempirical theories as well as empirical correlation expressions are summarized in uniform notation and are compared with each other and with the experimental. For normal impact on quasi-infinite targets two empirical correlation expressions are deduced which are more generally applicable than previous expressions. A qualitative description of the cratering process is given and realistic regions of impact are defined. Recommendations for future experimental and theoretical work are made.

Holmes, R. H., and Enos, W. F., "Medical Aspects of Body Armor Used in Korea," J.A.M.A. 155, 1477 1954

Hopkins, H. G. and Kolsky, H., "Mechanics of Hypervelocity Impact of Solids,"
4th Symposium of Hypervelocity Impact,
Volume I, APGC-TR-60-39 September 1960

Th

In general, the unsteady motion produced during the impact of solid projectiles and targets involves, in a highly complex manner, combinations of fundamentally different physical regimes characterized through the occurrence of elastic and plastic deformation, incompressible and compressible flow, and, in the limit, explosion conditions. A severe compromise is necessary between physical realities and mathematical complexities in theoretical studies of hypervelocity impact, and accordingly only a limited degree of precision is possible.

Hurlich, A., "Armor Plate,"
Watertown Arsenal
Watertown, Massachusetts
Report No. 710/451 July 1942

Ex, M, Thk, LV

Further studies of the mechanism of penetration of homogeneous armor plate by metallographic means of the nature of the deformation produced in 1/2" thick homogeneous rolled armor plate by caliber .30 armor-piercing bullets.

Johnson, D. K., Cannon, E. T., Palmer, E. P. and Crow, R. W., "Cratering Produced in Metals by High Velocity Impact,"
Department of Electrical Engineering
University of Utah
Technical Report UU-4 July 1959

Ex, M, Thk, LV

Steel spheres were accelerated to velocities up to 2.5 km/sec and impacted on targets of copper, lead, aluminum, magnesium, zinc, silver and 4140 steel. Volume, area and depth of the resulting craters are plotted as functions of projectile energy or momentum. Crater volume was found to be proportional to projectile energy. Area and penetration were dependent on projectile deformation as well as velocity.

Jones, A. H., Polhemus, J. F., Herrmann, W., "Survey of Hypervelocity Impact Information II,"
Massachusetts Institute of Technology December 1963

Ex, M, NM, Thk, Thn, HV, LV

More information which has been gathered since Volume I of this survey was published has been discussed. This pertains to impact on quasi-infinite targets, finite thickness targets, thin

plate targets and shielded targets. Data for impact into targets of the type described are presented in graphical form and compared with present theory. Also, data has been gathered for impact on composite targets. Recommendations for future experimental and theoretical work are made.

Kinard, W. H., et al., "Effect of Target Thickness on Cratering and Penetration of Projectiles Impacting at Velocities to 13,000 ft/sec,"
Langley Research Center
Langley Field, Virginia December 1958

Ex, M, LV, HV, Thn, Thk
This study tried to determine the effects of target thickness on the penetration and cratering characteristics for a target resulting from impacts in the 4000 ft/sec-13,000 ft/sec range. They used aluminum projectiles into aluminum targets and steel projectiles into aluminum and copper targets. Penetration was found to be a function of thickness provided that the penetration was greater than 20% of the target thickness.

Kinard, W. H. and Lambert, C. H., Jr., "An Investigation of the Effect of Target Temperature on Projectile Penetration and Cratering,"
NACA RM LS8E14, 1958, N 63-18043

Ex, LV, HV, M, Thk
Results of steel projectiles fired into copper targets at velocities from 5,000 to 11,500 ft/sec indicate that as the target temperature is increased the crater size also increases. Projectiles impacting targets heated to 900°F produced craters having as much as twice the volume of craters produced by projectiles of the same type impacting targets having a temperature of 80°F. It appears that the decreasing of the speed of sound in the target material as it is heated can be used as a parameter to predict the amount of increased cratering to be expected when targets are heated.

Kineke, John H., Jr., "Observations of Crater Formation in Ductile Materials,"
5th Symposium on Hypervelocity Impact
Vol. I, Part 2, October 1961

Ex, M, Thk
The model presented here is substantiated by the following experimental observations:

1. The crater size observations at various impact velocities in a number of target materials, and the crater size observations in the two aluminum alloys at various temperatures

indicate that the strength of the target material is the predominant factor in determining the final crater size in targets of ductile material.

2. The investigation of shock propagation gives evidence that the dynamic strengths of materials under hypervelocity impact substantially exceed those under static loading conditions, in targets of brittle materials.
3. The observations of crater growth show that craters are formed in periods of time long compared with those for the completion of the transient and steady-state regimes. They also substantiate the existence of a rebound in the crater dimensions in the latest stages of development.

Kinslow, R., "Properties of Spherical Stress Waves Produced by Hypervelocity Impact,"
ARO, Inc.
AEDC-TDR-63-197

Ex

A semi-empirical model derived which will, it is hoped, contribute to the understanding of the nature of waves and fractures in solids caused by hypervelocity impact.

The distance within a solid at which the shock wave slows down to an elastic wave is considered as the radius of a "cavity" to the surface of which a forcing function can be applied to produce an elastic wave similar to that produced by the impact of a high velocity projectile.

By the use of a high-speed computer, the characteristics of the forcing function are found which will produce the same effects as those caused by a projectile. This forcing function can be described by a mathematical series, each term being of the form for which the general wave equation can be solved. This permits the computation of particle displacement, particle velocity and principal stresses within the target.

Kolsky, H. and Shearman, A. C., "Investigation of Fractures Produced by Transient Stress Waves," Research, Vol. 2, p. 384, 1949

Kraft, J. M., "Surface Friction in Ballistic Penetration," J. Appl. Physics, Vol. 26, 1248 1955

Ex, M

The frictional adhesion between projectile and target during a ballistic penetration has been measured with a torsion-type

Hopkinson bar. The apparatus allows measurement of the torsional adhesion of a spinning projectile during target penetration. By assuming the friction resisting rotation to equal that resisting axial penetration, the energy loss due to friction was computed. The results show that the torque-time pattern during penetration of a "mechanically" clean projectile can be predicted with the assumption of a frictional energy loss just sufficient to keep the sliding surfaces at the melting temperature of the metal. Metallographic analysis of the target metal at the projectile interface gives a further indication of a molten interface. In these tests, sliding friction accounts for about 3% of the striking energy of the projectile; common surface contaminants, not necessarily special lubricants, reduce this loss to less than 1%.

Kramer, I. R. and Maddin, R., "Delay Time for the Initiation of Slip in Metal Single Crystals," Journal of Metals, Vol. 4, p. 197, 1952

Kreyenhagen, K. N. and Zernow, L., "Penetration of Thin Plates,"
5th Symposium on Hypervelocity Impact
Vol. I, Part 2
October 1961

Ex, M, Thn, HV

This paper discusses the process of penetration of thin plates by hypervelocity projectiles. In the experiments which will be described, aluminum alloy plates of 0.100" thickness are impacted by one gram titanium projectiles at velocities of the order of 5 km/sec. These conditions are in a regime where complete penetration occurs. The results of these experiments suggest a general model for such impact and penetration phenomena.

Kuhlmann, H. W., et al., "The Development of Laminated Armor,"
Battelle Memorial Institute for Watertown Arsenal, Watertown, Massachusetts
April 1949

Ex, NM, LV, Thn

Several laminates were prepared using plasticized polyvinyl chloride, polymethyl methacrylate and plaskon 920 as the binders for 2x2 basket-weave, 13-ounce nylon. The ballistic and physical properties of these laminates were studied in the hope of establishing some correlation between the two properties. It was found that polyvinyl chloride bonded laminates were generally superior to the other binders. However, bonded nylon was not particularly superior to unbonded nylon.

Maiden, C. J., Tardif, H. P. and Charest, J., "An Investigation of Spalling and Crater Formation by Hypervelocity Projectile,"
Annual General Mtg., Transaction, Vol. LXIV, pp. 140-149, 1961
(Canadian Mining and Metallurgical Bulletin, Vol. 54, February 1961)

Mallory, H. Dean, "Propagation of Shock Waves in Aluminum," J. Appl. Physics, Vol. 26, No. 5 May 1955

Ex, M

The velocity of shock waves in aluminum and the associated translational motions, produced by metal-metal impact have been determined by an electrical contact technique. The results obtained have been used to evaluate an equation of state for the metal.

Mayfield, E. B., and Rogers, J. W., "Cratering and Shock Wave Phenomena in Steel Plates at High Impact Speeds," J. Appl. Physics, 31:472-3, March 1960

Ex, M, Thn, LV

The impact of aluminum projectiles on steel plates for impact velocities of 2500 m/sec to 3000 m/sec and about 1100 m/sec was studied. Crater volume and penetration were measured. Shock wave velocity from the free surface was determined and the particle velocity calculated. For annealed 4130 steel plates impacted at 2750 m/sec average velocity, the average free surface particle velocity was 0.205 mm/μsec. Existing theory on cratering and penetration gave excellent agreement with the observed values.

McDermott, C. E., Cannon, E. T. and Crow, R. W., "Temperature Studies and Effects in Perforation of Thin Aluminum Targets,"
Department of Electrical Engineering
University of Utah
Technical Report UU-3, May 1959

Ex, M, Thn, LV

Steel spheres were accelerated to velocities of 2.5 km/sec and impacted on thin aluminum targets. These targets varied in thickness from 1/16" to 5/16". The targets were also tested at varying temperatures of 70°F, 200°F, 350°F and 500°F. The residual velocity was measured after perforation. It was found to be an increasing function of the target temperature.

McKenzie, R. I., Martin, F. F., and Kenworthy, H. M., "High Velocity Impact of Small Metal Spheres Upon Flat Metal Targets,"
3rd Symposium on Hypervelocity Impact February 1959

Ex, M, LV

A discussion of some of the data, analyses and observations associated with two series of special fragment-target impacts. Several expressions relating penetration and cratering with velocity and other parameters correlated to those data are introduced.

The range of velocities was from 1000 to 6000 ft/sec. The fragments were as small as 15 grains and as large as 7000 grains with selected sizes in between.

McQueen, R. G. and Marsh, S. P., "Equation of State for Nineteen Metallic Elements from Shock Wave Measurements to Two Megabars," J. Appl. Physics, Vol. 31, No. 7 July 1960

Ex, M

Plane wave explosive systems were used to accelerate thin metal plates to high velocities. Shock pressure resulting from the collision of these driver plates with a stationary target plate are approximately three times greater than in the driver plate. The photographic flash gap technique was used to record velocities associated with the shock waves. The new experimental data extend the Hugoniot loci into the one to two megabar region for 19 metallic elements: Ag, Au, Cd, Co, Cr, Cu, Mo, Ni, Pb, Sn, Th, Ti, Tl, V, W, Zn, Bi, Fe, Sb.

Mellecker, J. B. and Gailus, W. J., "The Light Armor Testing Laboratory and Research Relating Thereto,"
Monsanto Chemical Company
Vol. II December 1945

Ex, NM, LV, Thn

A discussion of glass and glass facial armor tests with velocities to 3,000 ft/sec. Glass alone when supported by some non-armor material such as artist's clay was found to absorb most of the energy of the projectile (7/32" steel sphere) penetrating it. Testing equipment and procedures along with graphs of data and pictures of tests are included in this report.

Meyer, E. A. and Jansen, N. I., "Information Regarding the Energy Absorbing Characteristics of Materials for Utilization in Armor,"
Bjorksten Research Laboratories, Inc. June 1957

Ex, E
Deals with errors in speed measurements in firing range.

Morris, C. R., Partridge, W. S. and Cannon, E. T., "Perforation of Thin Aluminum Targets,"
Technical Report UU-1 August 1958

Ex, M, LV, Thn, E
Steel spheres were accelerated to a velocity in the range between 0.5 km/sec and 2.63 km/sec and were impinged normally upon thin targets of aluminum. The amount of energy lost by a pellet in perforating a target was found to be directly proportional to the kinetic energy of the impinging pellet. The minimum amount of energy required for a pellet to perforate aluminum was found to be an increasing function of target thickness. It was also found that the hole diameter increased as the impact velocity increased.

National Bureau of Standards, "Development of Personnel Armor,"
Special Summary Report 9A129 covering period July 1, 1954 to May 31, 1955

Discusses small squares, ribbons, etc. of plastic.

O'Brien, J. L. and Davis, R. S., "On the Fracture of Solids Under Impulsive Loading Conditions,"
Response of Metals to High Velocity Deformation Proceedings
Estes Park, Colorado 1960
Vol. 9, p. 371, Metallurgical Society Conferences, Interscience Publishers

Ex, M
A discussion of scabbing or spalling phenomena that is associated with the reflection of a compression stress wave from a free surface, both in terms of the previous work in this field and results obtained by the authors. In addition, multiple-pellet technique for obtaining the pressure profile of an incident compression shock is discussed. The reported dependence of stress for fracture as a function of the intensity of the incident compression at the position of fracture is explained in terms of errors introduced by the techniques used to measure shock profiles.

Olcott, J. S., "Chemical Strengthening of Glass," Science, Vol. 140, No. 3572, 14 June 1963

Ex, NM

Through the years glass has been particularly noted for its transparency, refractoriness and chemical durability. Unfortunately, because of it fragility, the use of glass has been limited whenever even modest forces might be applied to it. During the past few years, however, steps have been taken by glass scientists to reduce the vulnerability of glass to fracture. Annealing, the first step in making glass a useful material, has enabled us to make articles with strengths adequate for satisfactory service. Physical tempering provided the next big advance, permitting strengths more than three times those of annealed glass in simple shapes. Today, chemical strengthening is a real possibility for producing glass articles, regardless of design, more than three times the strength of physically tempered ware.

Olshaker, A. E. and Bjork, R. L., "Hydrodynamics Applied to Hypervelocity Impact; II. The Role of Melting and Vaporization in Hypervelocity Impact," 5th Symposium on Hypervelocity Impact Vol. I, Part 1, Nonr-(G)-0020-62(X) October 1961

Th

During the portion of a hypervelocity impact where tremendous pressures are present the strength and latent heat of fusion do not affect the process in an important way. However, in the later stages of the impact when the pressure and internal energy fall to a low level, the condition of the material can become important.

When the material is shock loaded the entropy undergoes a substantial increase, proportional to the third and higher powers of the shock strength. Stronger and stronger shocks level to fusion, heated liquid, vaporization and superheated vapor of the material as the final state. This paper discusses the final condition of the material as a function of shock strength.

Olshaker, A. E., and Bjork, R. L., "Hydrodynamics Applied to Hypervelocity Impact, I. Scaling Laws for Dissimilar Materials,"

Th

The fundamental equations of motion of hydrodynamics are applied to an impact process. From these the Hugoniot relationship is derived. Using the equations of state as found in the Los Alamos

tests the shock process is described. Using the information obtained from these equations scaling laws were arrived at that correlated crater size with the various projectile-target combinations.

Orowan, E., "Energy Criteria of Fracture,"
Welding Journal Research Supplement, p. 1 March 1955

Orowan, E., "Condition of High Velocity Ductile Fracture,"
J. Appl. Physics, Vol. 26, No. 7, p. 900 July 1955

Th
The Griffith energy criteria, dW = -dU (dW = crack propagation work, -dU = released elastic energy) cannot be applied to essentially ductile fractures. In particular, it does not represent the condition of rapid ductile fracture propelled by the elastic energy of the specimen. The condition of such fractures is $d^2W/dX^2 = -d^2U/dX^2$, where X is the plastic extension accompanying the propagation of the crack.

Paca, Francis B., "The Response of Materials to Dynamic Loads,"
U. S. Army Engineer Research and Development Laboratories
Fort Belvoir, Virginia

Th
A review is made of the static and dynamic response of materials to stress. The action of stress and strain waves involved during impact is discussed in terms of wave propagation under various boundary conditions. Cottrel's dislocation theory of delayed yielding is discussed. The test apparatus used in the application of dynamic loads are reviewed and their characteristics analyzed. A simplified method is presented for conducting dynamic loading tests on materials of various kinds and on materials having a very high strength.

Pack, D. C., Evans, W. M. and James, H. J., "The Propagation of Shock Waves in Steel and Lead,"
Proceedings, Physical Society, Vol. 60, p. 1 1948

Palmer, E. P., "Penetration and Cratering,"
University of Utah Technical Report UU-7, October 13, 1961

Ex, Th, M, LV, Thk, Thn, E
This report is the summary of work that has been carried out in the following five phases:

1. A systematic investigation of the influence of target properties and projectile properties in high-velocity cratering and the formulation of empirical impact laws describing the results.

2. An investigation of penetration and perforation of thin targets of aluminum and glass.

3. An experimental and theoretical investigation of the transient behavior in cratering, including an investigation of energy distribution and flow and wave motion.

4. A detailed theoretical and experimental investigation of elastic and plastic wave propagation in a rod.

5. An investigation of impact at velocities up to 25 km/sec utilizing micron-sized spray particles.

Partridge, William S., Vanfleet, Howard B., and Whited, C. R., "Crater Formation in Metallic Targets,"
J. Appl. Physics, Vol. 29, No. 9 September 1958

Ex, M, LV, Thk

Spheres of copper, lead, tin, iron, aluminum, zinc, silver, and lead-tin alloys were accelerated to velocities of 0.75 to 2.25 km/sec and impacted normally upon targets of the same material as the pellets. Conditions were maintained so that pellets lost no mass before striking the target. The target mass was large compared to the mass of the pellet, so the targets could be considered semi-infinite.

The volume of the crater produced was found to be directly proportional to the kinetic energy of the pellet in the energy range investigated.

The penetration varied linearly with the velocity or momentum of the pellet. The area of the crater as measured in the plane of the original surface of the target was found to be directly proportional to the momentum of the pellet at the time of the impact.

In the case of the lead-tin alloy series, a correlation was observed between the crater parameters, the phase diagram of the alloys, and various functions of the pellet mass and velocity for the following series of alloys: 100% lead, 90% lead, 10% tin, 10% lead, 90% tin and 100% tin.

Partridge, William S. and Clay, Wallace G., "Studies of High-Velocity Impact in Wax,"
J. Appl. Physics, Vol. 29, No. 6 June 1958

Ex, NM, LV, Thk

Penetration of wax pellets into wax targets was found to vary linearly with the cube root of the pellet mass and the pellet velocity up to velocities in excess of twice the sonic velocity in the wax target. The crater area varies directly as the impact velocity, but there is a marked increase in the constant of proportionality above the target sonic velocity. The volume of the crater per unit energy of the pellet was found to be 2.23×10^{-8} m^3/joule for the lower velocity range and above the target sonic velocity the value was found to be 2.75×10^{-8} m^3/joule.

It was observed that a large part of the crater volume is created by deformation of the target material and that only a small part is due to ejection of the target material.

Percy, J. H., "Wave Propagation in Uniaxial Strain,"
Proceedings of Symposium on Structural Dynamics under High Impulse Loading
May 1963

Th

Interest in this topic centers on the constituative equation or behavior of materials under the extreme conditions of high impulse loading. Recent and current work in the field is treated generally and one area, the elastic-plastic behavior of aluminum at comparatively low pressures, is considered in detail.

Petterson, D. R., Stewart, G. M., "Dynamics of Body Armor Materials Under High Speed Impact; Part IV. Nominal Dynamic Stress-Strain Curves from Strain-Position Distributions,"
Textile Research Journal, 30, 422, 1960

Polaroid Corporation, "Investigation of the Energy Absorption Characteristics of New Polymeric Materials,"
Final Report, Contract DA 19-129-QM-209.

CONFIDENTIAL

Poncelet, E., "Fracture and Comminution of Brittle Solids,"
Metals Technology 11, 1, 1944. Also known as Technical Publication No. 1684 of the Am. Inst. Min. and Met. Eng.

Recht, R. F. and Ipson, T. W., "Ballistic Perforation Dynamics,"
Journal of Applied Mechanics
Paper No. 63-APM-24 (ASME) September 1963

Th, Ex

Analytical equations of the types required to define ballistic perforation dynamics are developed. These equations concern both blunt and sharp nosed fragments perforating plates normally and at oblique impact angles. Residual velocities are defined in terms of magnitude and direction. Analytical models and confirming experimental data, which are presented here, specifically concern the ballistic velocity-impact range to about 25% of the velocity of longitudinal sonic waves in the material.

Reed, E. L., and Kruegel, S. L., "Correlation of Microstructure and Ballistic Properties of Armor Plate,"
Watertown Arsenal
Watertown, Massachusetts
Report No. 710/261 July 1938

Ex, M, Thn

A correlation of microstructure and ballistic properties of all homogeneous armor plate on hand at Watertown Arsenal. It was found that spalling was caused by laminations, carbides in definite chains in grain boundaries and martensitic structure.

Rice, M. H., Walsh, R. G. and Walsh, J. M., "Solid State Physics - Advanced in Research and Applications. Compression of Solids by Strong Shock Waves,"

Th

Using the basic relations of fluid mechanics and experimental data obtained from impulse loading the equations of state were determined for many pure metals. Two wave structures resulting from phase-changes are discussed. The methods of arriving at the experimental data are discussed also.

Rinehart, J. S., "Some Quantitative Data Bearing on the Scabbing of Metals Under Explosive Attack,"
J. Appl. Physics, Vol. 22, p. 555, (UU) 1951

Rinehart, J. S., "Scabbing of Metals Under Explosive Attack: Multiple Scabbing,"
J. Appl. Physics, Vol. 23, p. 1229 (UU) 1952

Rinehart, J. S., "Discussion of Paper by D. S. Wood, 'On Longitudinal Plane Waves of Elastic-Plastic Strain in Solids,'"
Journal of Applied Mechanics, Vol. 20, p. 307 1953

Rinehart, J. S. and Pearson, J., "Behavior of Metals Under Impulsive Loads,"
American Society of Metals
Cleveland, Ohio 1954

Ex, M, NM

This book discusses the character of impulsive loading, indicates the conditions under which such loading can develop, and describes the main phenomena that become involved when materials, primarily metals, and system of material bodies are subjected to rapidly applied loads of short duration.

Riney, T. D. and Chernoff, P. R., "Inertial, Viscous and Plastic Effects in High Speed Impact,"
5th Symposium on Hypervelocity Impact
Vol. I, Part 1, Nonr-(G)-0020-62(X) October 1961

Th

When an ultra-high-speed projectile strikes a target a strain rate which depends on the impact velocity is imposed on the projectile and target materials. The resulting flow of the materials will be resisted not only by the inertial forces, but also by the dynamic yield strength of the materials and by viscosity stresses with magnitudes which depend upon the strain rate. The only serious attempt to calculate the phenomenology of hypervelocity impact from basic principles has considered the medium to be a perfect fluid and consequently neglected the strength and viscosity effects. Since the predictions from the perfect fluid model are found to differ from the extrapolated results of hypervelocity impact tests, one is led to consider the problem anew in order to formulate a mathematical model which takes into account the inertial, viscous and strength effects.

Rockowitz, M., Carey, C. A., Dignam, J. F., "Hypervelocity Impact of Heated Copper,"
5th Symposium on Hypervelocity Impact
Vol. I, Part 2, October 1961

E, M, HV, Thk

Hypervelocity impact of semi-infinite blocks of OFHC-type copper has been made with aluminum, chrome alloy steel and tungsten carbide projectiles of 1/4 gram mass at velocities up

to 6.5 km/sec. The target temperature varied between room temperature and 1600°F. All impacts were made normal to the target surface.

An investigation is made to determine how the importance of target temperature and mechanical properties vary with increasing projectile velocity. Also, a correlation of the variation of energy/volume and target tensile strength is made.

Rutgers University, "Investigation of Low Density and Reinforced Ceramic Structures for Application in Helmet and Body Armor,"
Final Report, Contract DA 19-129-QM-1974

CONFIDENTIAL

Schipper, J. F., "A Model of Non-explosive Impact,"
5th Symposium on Hypervelocity Impact
Vol. I, Part 1, Nonr-(G)-0020-62(X) October 1961

Th
The model of impacting to be constructed here consists essentially of a sequence of time regimes, not always non-overlapping.

The first time regime begins at the moment the projectile first encounters the target. At t=0 both target and projectile begin to deform, according to the relation between their respective densities and compressibility factors.

When the impact is supersonic, the velocity of impact is greater than the acoustic velocity of either projectile or target material. The second time regime is taken to begin at the instant T_1 at which the velocity of the advancing front has just become sonic in the projectile.

The third regime (and also the fourth), is taken to begin at the time T_2 which the temperature in at least one local domain is "just sufficient" for melting to begin locally. It is possible that within this time regime, the shock waves reflected from the rear boundary of the projectile will return, adding to the complexity of the reaction. Because of the high pressure present, this melted material will be extruded, flowing along the small space between the boundaries of the respective unmelted parts of the bodies and up the sides of the crater produced.

Shand, E. B., "Fracture Velocity and Fracture Energy of Glass in the Fatigue Range,"
American Ceramic Society Journal 44:21-26, January 1961

Ex, NM

A method is developed for determining crack velocities from the stress-time curve of fracture. Velocities of glass broken in air and in a vacuum converge at a value between 1 and 10 mm/sec. This convergence is considered to be the upper limit of the fatigue range. Fracture energy has been computed in terms of strain energy release rates. For glass broken in air under low stresses this energy is about equal to the surface energy of the glass, but when in vacuum it is fifteen times greater. At the upper limit of the fatigue range it is thirty times greater; whereas, at the terminal velocity of fracture it is of the order of fifty times greater. It is concluded that surface energy must constitute only a small part of the energy absorbed in the fracture process. This excess energy has a pronounced influence on the fracture process and on the measured strength of glass.

Shand, E. P., "Correlation of Strength of Glass With Fracture Flaws of Measured Size,"
American Ceramic Society Journal, 44:451-5 September 1961

Ex, NM

The purpose of this study was to develop a method of producing a single small crack on a glass surface which would become the initiating flaw in the fracture process. Techniques for measuring the dimensions of the flaw also formed an essential part of the study. The cracks were formed by pressing a wedge-shaped tungsten carbide point against the glass. Measurements were made from visible patterns found on the fracture surface after the glass was broken. Strict adherence to carefully worked out procedures was found to be essential for obtaining satisfactory cleaved cracks.

Smith, J. C., Blandford, J. M., and Schiefer, H. F., "Stress-Strain Relationships in Yarns Subjected to Rapid Impact Loading. Part VI: Velocities of Strain Waves Resulting from Impact,"
Textile Research Journal, 30, 752, 1960

Smith, J. C., "Characterization of Textile Yarns for Use Under Ballistic Impact Conditions,"
U. S. Department of Commerce
Symposium on Personnel Armor
Naval Research Laboratory 4-5 October 1961

Smith, J. R., McCrackin, F. L., and Schiefer, H. F., "Stress-Strain Relationships in Yarns Subjected to Rapid Impact Loading: III. Effect of Wave Propagation."
Journal Research National Bureau of Standards, 55, 19, 1955
Textile Research Journal, 25, 701, 1955

Sodha, M. S. and Jain, V. K., "Physics of Armor Penetration."
J. Appl. Physics, 29:1769-70 December 1958

Summers, J. L., "Investigation of High-Speed Impact: Regions of Impact at Oblique Angles."
NASA TN D-94 October 1959

Ex, M, LV, Thk
Small metal spheres were fired into copper and lead targets at velocities up to 11,000 ft/sec. Target penetration and cavity volume can be correlated as functions of the ratio of projectile to target density and the ratio of impact velocity to speed of sound in target material. Impact for which the correlation equations apply is described as occurring in the fluid-impact region. This type of impact as well as other types is discussed. Penetration for impact at oblique angles is correlated with that for normal impact on the assumption that the component of velocity parallel to the target surface does not contribute to target penetration.

Summers, James L. and Charters, A. C., "High Speed Impact of Metal Projectiles in Targets of Various Materials."
Proceedings of 3rd Symposium on Hypervelocity Impact, February 1959

Ex, M, LV, HV, Thn
A summary of some results in the field of high-speed impact obtained at Ames Research Center. The projectiles were metal spheres and rods to determine, for engineering purposes, the damage caused by small bodies such as meteoroids impacting against a surface such as a skin of a satellite or space vehicle. Several different metals were employed as target materials. Impact at both normal and oblique angles were studied. Projectile velocity ranged from a few hundred feet per second to nearly 12,000 ft/sec.

Susich, G., Dogliotte, L. M., and Wrigley, A. S., "Microscopical Study of a Multilayer Nylon Body Armor Panel After Impact,"
Textile Research Journal, Vol. 28, p. 361 May 1958

Ex, NM, LV, Thn

A body armor panel consisting of twelve identical layers of 2x2 basket-weave nylon fabric was investigated after impact by a fragment simulator .22-caliber steel missile in the range of 330-420 m/sec (1100-1400 ft/sec) striking velocities. The kinetic energy of the projectile was either slightly higher or lower than that the panel could absorb (706,000 g-cm).

Completely and partially penetrated holes were investigated. The area surrounding the bullet holes was studied to learn about the various types of deformations and damages in each layer.

Cross sections at various levels were made. It was recognized that the permanent damage was localized to a small area close to the path of the projectile.

After separating the panel into individual layers, the stoppage of the projectile was studied. There was some damage due to heat of impact. Stress propagation was prevented by cross yarns.

Szebehily, V. G., "Hydrodynamics Impact,"
American Soc. Naval Engineering Journal, 72:137-41, February 1960

Trent, D. L., "Meteoroid Impact on Shielded Space Vehicles,"
ASME 63-AHFT-69

Th, Thn

The design of a minimum weight reliable meteoroid shield must be based on a knowledge of the mechanisms of hypervelocity impact, because of the inability of present experimental equipment to duplicate meteoroid velocities. This study consists of a preliminary analysis of the problem of cratering and penetration using a hydrodynamic model. An analysis is made of the impact of a solid projectile on a metal plate. Conditions for penetration of the shield and destruction of the projectile are explored. Various materials are compared for use in meteoroid shields and recommendations are made for material selection.

Thomson, W. T., "An Approximate Theory of Armor Penetration,"
J. Appl. Physics, 26:80, 1955

Th, E, Thn

The problem of armor penetration of thin plates is considered from a quasi-dynamical approach. Equations are derived for the energy dissipation due to plastic deformation and for heating of the projectile target interface. Both the conical and the ogival head are considered in the application of the general equations.

Van Valkenburg, M. E., Clay, Wallace G. and Huth, J. H., "Impact Phenomena at High Speeds,"
J. Appl. Physics, Vol. 27, No. 10 October 1956

Ex, M, NM, LV, Thk

A study of high speed metal-to-metal impact in the velocity range 1 to 5 mm/μsec using 1/8" diameter spherical pellets is described. Pellet materials include aluminum, magnesium, steel, brass, lead and zinc. Experiments relating to the mechanisms of cratering and the perforation of thin targets are presented. For the 1/8" diameter spherical pellets, it is found that the volume of the crater per unit energy of the impacting pellet is essentially constant for each material and that the penetration is proportional to the velocity of the pellet so long as the pellet velocity is less than the velocity of sound in the target material. An attempt to model very high speed impact by using soft wax targets in which the sonic velocity is less than the impacting velocity is outlined.

Vitali, R., Becker, K. R., and Watson, R. W., "Perforation of Finite Targets by High Velocity Projectiles,"
5th Symposium on Hypervelocity Impact
Part 2, Vol. I October 1961

Ex, M, Hv, Thn

The increasing demand for information pertaining to the effects of hypervelocity impact on targets of finite thickness has led to the following investigation of target perforation by a small, high velocity projectile. The behavior of five different target materials - lead, aluminum 250, 2024SO and 2024T-3, and magnesium AZ51X, B90-46T - has been investigated at two angles of attack, 0 degrees and 60 degrees. The projectile employed throughout is a 0.024 gram steel cylinder, projected at a velocity of 3.2 km/sec. The target materials varied in thickness, ranging from 0.031" to 1.0". Graphs are presented which

illustrate the following: hole dimensions as functions of target thickness, mass of spall as a function of target thickness, and the spatial distribution of the spall fragments.

von Karman, T. and Duwez, P., "The Propagation of Plastic Deformation in Solids,"
J. Appl. Physics, Vol. 21, p. 987 1950

Whitlock, T. W., "Investigation of Variables Effecting the Performance of Light Weight Armour,"
Midwest Research Institute
Final Report, Contract DA 23-072-ORD-815, W.A.L. File 710/1049, June 1955

CONFIDENTIAL

Wood, D. S. and Clark, D. S., "The Influence of Temperature Upon the Time Delay for Yielding in Annealed Mild Steel,"
Transactions, American Society for Metals, Vol. 43, p. 571, 1951

Yuan, S. W. and Bloom, A. M., "An Analytical Approach to Hypervelocity Impact,"
North American Aviation, AIAA Summer Meeting June 1963

Th
Based on the assumption that the regime of fluid impact exists when a projectile strikes a target, an expression has been developed for a penetration parameter as a function of an impact velocity parameter. This expression is obtained from the simultaneous solution of one-dimensional equations of a viscous compressible fluid. Hugoniot equations of state are used in this analysis as derived by Walsh, Rice and McQueen. Good agreement between theory and experimental data is obtained.

Zaid, M., "An Analytical Approach to Hypervelocity Impact Mechanics,"
4th Symposium of Hypervelocity Impact
APGC-TR-60-39, Vol. III September 1960

Th
A presentation of a rational theory of target perforation by ultra-high speed penetrators. The over-all approach is the same as that taken previously by the author in the theoretical and experimental studies of thin plate perforation by non-deforming projectiles; that is, the perforation process is idealized to retain only its essential characteristics. Then, based upon this idealization, a mathematical description is written and solutions obtained. In order not to

obscure the basic concepts with solution and techniques, only the derivation of the equations of motion is presented in detail. The case considered is that of normal perforation of a deformable target by a non-deformable cylindrical penetrator traveling at hypervelocities; its extension to the deformable penetrator of other geometry and obliquity or target thickness being directly obtainable from the techniques presented in this paper.

Zaid, M., "Penetration by Hypervelocity Particles,"
5th Symposium on Hypervelocity Impact
Vol. I, Part 1, Nonr-(G)-0020-62(X) October 1961

Th, Thk

In this paper additional equations are presented for the solution to the problem of a non-deformable ultra-high speed penetrator striking a semi-infinite deformable target. These, together with the ones of a previous paper, provide a complete mathematical description of a penetration model. Based on these equations, and on an assumed stress-velocity relationship, various "growth" laws are postulated and solutions for penetration distance, velocity and time history are obtained. From these it is seen that although the phenomenon is sensitive to the exact magnitude of physical parameters, it is much less sensitive to a variation in the formulation of the "growth" law.

The paper suggests many areas in which experimental work would be fruitful, and additionally provides a model capable of extension to the deformable-penetrator deformable-target problem.

Zaid, M. and Paul, B., "Mechanics of High Speed Projectile Perforation,"
Franklin Institute Journal, Vol. 264, pp. 117-126, 1957

Thn

The problem of perforation of thin plates by high speed projectiles is considered from a momentum viewpoint. Equations representing the magnitude and direction of forces, velocity, etc. as a function of penetration distance are derived for the conical projectile under normal impact. Good correlation between the theory and experiment is obtained. A model of thin plate perforation by conical projectiles is analyzed.

Zaid, M. and Paul, B., "Normal Perforation of a Thin Plate by Truncated Projectiles,"
Franklin Institute Journal, Vol. 265, p. 317 1958

Ex, Thn

The general solution to the problem of perforation of thin plates by high speed projectiles is extended to truncated conical and ogival projectiles. The velocity distance relationships are obtained for these general cases, and the forces are evaluated for pointed ogival projectiles. Comparison of theory and experiment is made and the agreement is satisfactory.

Zaid, M. and Paul, B., "Oblique Perforation of a Thin Plate by a Truncated Projectile,"
Franklin Institute Journal, Vol. 268, p. 24 1959

Ex, Thn

The author's previous analyses of normal perforation of thin plate by high speed projectiles are generalized to include truncated cones, at oblique striking angles. A complete velocity-displacement history is obtained for the most general case. Results are presented in graphical form.

Zener, C., "Mechanism of Armor Penetration,"
Watertown Arsenal
Watertown, Massachusetts
Report No. 710/454 September 1942

Ex, Thn

A study of the types of plate reaction to projectile impact. For striking velocities near the ballistic limit the elastic displacement of plate may be calculated and about 20% of the projectile's energy is dissipated by elastic waves in plates of thicknesses equal to the projectile's caliber, the fraction of energy dissipated decreases rapidly as the plate thickness increases. The shear plugs are discussed and the stress system is reconstructed. Plastic deformation is also discussed.

Zener, C., "Mechanism of Armor Penetration,"
Watertown Arsenal,
Watertown, Massachusetts
Report No. 710/492 May 1943

Ex, Thn

A study of the forces which act upon projectiles during armor penetration, and the effects thereof. Friction was found to have

negligible effect during armor penetration. An estimate has been made of the forces which arise from the inertial resistance of the plate material. The shape of the ogive and the resultant forces are also discussed. When the projectile penetrates in a ductile manner by pushing the plate material aside, the force needed increases as the plate hardness increases.

Zener, C., "Mechanism of Armor Penetration,"
Watertown Arsenal
Watertown, Massachusetts
Report No. 710/492-1 March 1944

Ex, M, Thn

Examples of shatter are presented, and the mechanism of the phenomenon is analyzed. A correlation was made by means of the stress-strain curves of the projectile steel, the expansion of the bourrelet with the hardness of plate, the striking velocity, and the hardness of the projectile.

Zener, C., "Mechanism of Armor Penetration,"
Watertown Arsenal
Watertown, Massachusetts
Report No. 710/492-2 August 1944

Ex, Thn

A method is outlined for computing the stresses and the deformation in armor during projectile impact. The primary problem in this computation is the evaluation of the effect of the plate material's inertia. Two approximations are made; the first, the force acting upon the plate is assumed to be so distributed as to give rise to no localized plastic deformation. The second is the method of support to give the velocity of the plate and the bending moments which can be computed in the first approximation. Examples are given of the effect of wave propagation both in the plate and in the projectile.

IV. PHASE II - A THEORETICAL STUDY OF LOW VELOCITY PENETRATION PHENOMENA

ABSTRACT

A new formulation of elasto-plastic rate-dependent material behavior is discussed. A numerical method and computer code (FORTRAN IV for IBM-7040) have been developed for the determination of two-dimensional displacement fields in large deformation impact situations. Preliminary numerical results are presented for the collision of two identical aluminum bars.

1. INTRODUCTION

1.0 Introduction to the Over-all Problem

This report presents a review of the initial work on a much larger problem. The over-all investigation has three principal goals:

1. The construction of a theory and computational scheme for the quantitative prediction of low velocity impact phenomena (when the material properties and geometry are given).

2. The determination of the dynamic properties of various materials of interest from the theoretical interpretation of experimental data.

3. The design of materials and geometries for various types of protective armor.

The theoretical method for the quantitative prediction of impact phenomena must be sufficiently general to permit the solution of systems which are complicated enough to be of practical use. It demands that the following should be accounted for:

1. Large deformation gradients necessitating the use of nonlinear geometric theory.

2. General, nonlinear (but continuous), rate dependent, elasto-plastic stress-strain relations.

3. Boundary conditions of sliding and nonsliding surfaces in contact.

4. Various geometries: Impacts of projectiles having rather arbitrary cylindrical profiles impacting into multi-layered targets.

The theory of material phenomena is presently unsettled. There is much disagreement concerning the proper qualitative nature of the theory.

With the limitations of current mathematics, computations of practical interest are exceedingly difficult, and subject to some considerable inaccuracies. One of the major goals of this project is to develop mathematical tools for the solution of more general mathematical models arising from various physical theories of material behavior. Clearly, this must be done before any physical theory is of practical utility.

1.1 Introduction to the Particular Problem of This Study

This study is in three parts, the first of which is now completed and is described in this report.

An outline of the particular goals of the project is given below. Parts II and III are included here to indicate the direction of future work.

Part I

1. Review of physical theory and construction of a simple physical model.

2. Mathematical formulation of the physical model.

3. Development of computational methods for solving mathematical models giving the time-dependent displacement and velocity fields within impacting materials.

Part II

1. Extension and refinement of the computational methods.

2. Verification of the computational techniques and mathematical model by comparing the theoretical calculations for a relatively simple model with classical results (where possible) and experimental data. elastic only

3. Extension of the mathematical model and computational scheme to the case of simultaneous elastic and plastic forces.

4. Theoretical calculations for several models that will be simulated experimentally.

5. Deduction of the proper form of the stress-strain relations of several materials by adjusting the numerical parameters in the mathematical model until the theoretical calculations coincide with the actual experiments.

Part III

1. Extension of the computational scheme to the more complicated geometries of practical interest.

2. Theoretical calculation of various impact configurations over time periods covering an entire impact or penetration (using the experimentally derived stress-strain relations from Phase II, step 5).

3. Interpretation of the results of step 4 to better understand the influence of various material properties and geometrical structures on impact and penetration phenomena.

1.2 Preliminary Results and Progress

The physical theory of materials has been reviewed and the effects we consider pertinent to the problem have been isolated.

We have expressed these effects in a novel, but convenient mathematical form. The continuum form of the mathematics was converted to a discrete variable version for computational reasons.

Considerable work was necessary to develop a numerical method and computer code for solving the discrete variable model. The computer code is now performing properly in the calculation of the two-dimensional displacement and velocity fields for the impact of two prisms.* The computer code must now be refined and optimized for further studies.

The displacement and velocity fields in the two prisms correspond quite well with extrapolated classical theory. Our greatest interest at this time is the further improvement of the shock behavior and the running time of the computer code. Then the code will be extended to handle simultaneous elastic and plastic stresses and strains.

The work thus far shows the basic feasibility of our numerical method in handling nonlinear impact problems.

---

* The problem has been reduced from three spatial coordinates to only two by the use of symmetry relations. Nonsymmetrical problems in three dimensions pose no particular theoretical difficulties, but at present only the largest electronic computers could achieve a numerical solution.

2. CONTINUUM THEORY

2.0 The Important Mechanisms in Low-Velocity Impacts

All properties of a material may ultimately be traced to its atomic and molecular structure. Unfortunately, the currently limited understanding of the relation of molecular and macro physical theories does not yet permit the accurate derivation of macro properties from hypothesized molecular structure. Therefore, molecular theory can be used only as a qualitative guide in planning a program to describe and measure material properties on the macro level.

We have somewhat arbitrarily divided the principle effects in low velocity impacts into generic classes. These are listed approximately in order of their relevancy.

1. Elastic Deformation
2. Plastic Deformation
3. Fracture and Fragmentation
4. Spray Particles and Other Ejecta
5. Sliding Interface Friction
6. Shock Heating
7. Change of Crystal Structure
8. Change of Phase
9. Chemical Reaction
10. Optical Radiation

This report is limited to the first three (and mainly the first two) effects. The remaining topics are either of minor importance or are too complicated to be treated adequately at this time. Work on effects four and five is to be taken up later in the project.

2.1 Geometrical Description of Material Effects

Elasticity, plasticity, etc. will be described in terms of the deformation of an infinitesimal cube. It can be shown that this approach leads to an invariant formulation in the tensor sense.

In the initial undeformed state, the material points are referred to an orthonormal vector basis $\vec{I}_i$.* Every material point P is associated with a position vector $\vec{P} = z^i \vec{I}_i$.

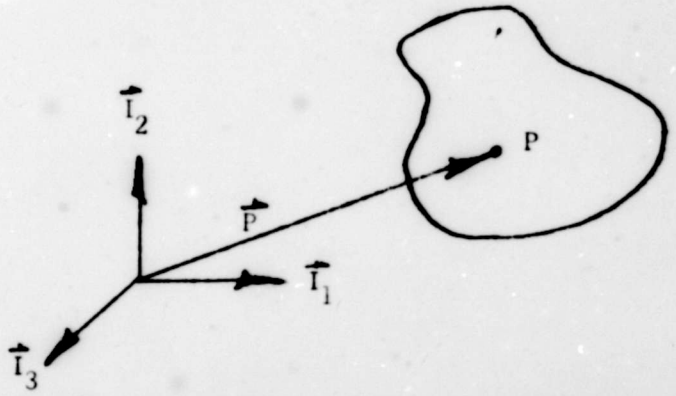

At each mass point P, a set of three infinitesimal orthogonal vectors $\vec{S}_i$ are chosen to represent the sides of an infinitesimal parallelepiped.

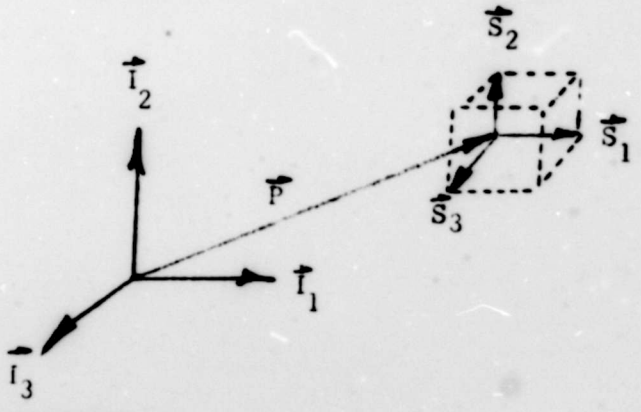

---

* See Appendix C for an explanation of the coordinate system conventions used in this report.

The infinitesimal side vectors are chosen parallel to the basis $\vec{I}_i$ so that $\vec{S}_i = dz^i \vec{I}_i$.

At later times the $\vec{S}_i$ are transformed in $\vec{s}_i$ which describe a deformed parallelepiped. The locally linear transformation connecting $\vec{S}_i$ and $\vec{s}_i$ is

$$\vec{s}_j = B_j^{\ i} \vec{S}_i$$

$$B_j^{\ i} = \frac{dY^i}{dY^j}$$

$\vec{S}_i$ basis $\qquad$ y^i coordinates

Y^i coordinates $\qquad$ $\vec{s}_j$ basis

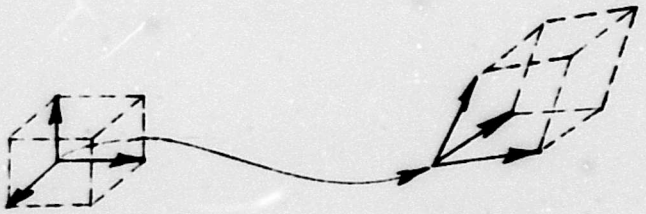

Initial $\qquad$ Deformed

The specification of the $\vec{s}_i$ basis (as a function of time) in terms of the $\vec{S}_j$ basis completely describes the geometrical deformation, and is therefore equivalent to the conventional strain tensor. The strain tensor is easily expressed in terms of $B_i^{\ j}$. However, the parallelepiped concept is much more intuitive.

Since the $\vec{S}_j$ are defined to be orthogonal and normalized, $B_i^{\ j}$ may be simply expressed as

$$B_i^{\ j} = \vec{s}_i \cdot \vec{S}_j \ . \qquad B_i^{\ j} \text{ is not a tensor.}$$

The usefulness of $B_i^{\ j}$ arises from the fact that the stress vectors $\vec{M}_i$ in the $\vec{s}_i$ basis are

$$\vec{M}_i = a^{\underline{i}} \vec{s}_{\underline{i}} = a^{\underline{i}} B_{\underline{i}}^{\ j} \vec{S}_j$$

as a consequence of conservation of momentum applied to an infinitesimal parallelepiped. The $\vec{s}_i$ are called the image vectors. The a^i are scalar functions which determine the relation between deformation and stresses. The a^i presumably are functions of the image vectors, time derivatives and perhaps integrals. We chose not to make implicit use of the stress vectors in the stress-strain relation; i.e., the stress vectors are given explicitly in terms of functions of the image vectors. This suffers no real loss in generality and is more convenient computationally.

Graphically, the forces on an infinitesimal parallelepiped are always parallel to the adjacent sides and act through the center of each side.

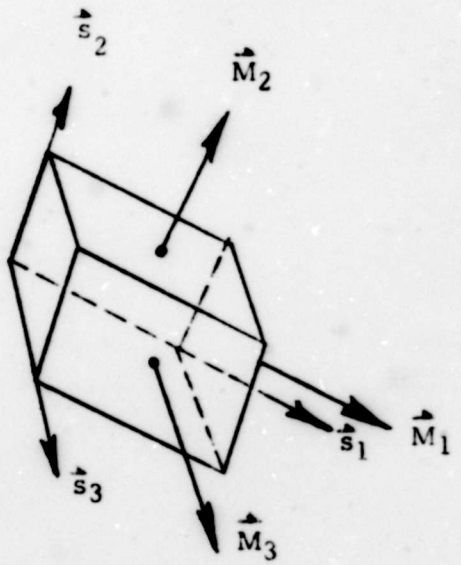

2.2 Isotropic Stress-Strain Relations

Any dynamic stress-strain relation must certainly reduce to the classical static form as the strains and time rates go to zero.

The volume of a deformed infinitesimal cube is (5,50)*.

$$V^2 = \left| \vec{s}_i \cdot \vec{s}_j \right|$$

$$V = \sqrt{|s_{ij}|}$$

where s_{ij} is the metric derived from the basis $\vec{s}_i$.

The stress-strain law of a material is conveniently stated in terms of the volume and side length changes and their time rates. The various molecular theories of materials seem to indicate that these quantities are of fundamental importance. Therefore, material forces may be visualized as arising from volume effects and side extensions. In isotropic media, this argument leads to two scalar functions: one for the volume effect and one for the extension effect.

The obvious place to start building a stress-strain relation is with the static, linear results. As an infinitesimal cube is deformed, forces arise as a result of the stretching or extension of its sides. For small variances these forces are assumed to be linear with side length change and the proportionality constant is the classical Young's modulus. The "shear" forces arise from volume change effects. Volume change forces are also assumed (for the moment) to be linearly dependent on the volume change. Expressed mathematically,

$$a^i = \left[\frac{1}{L_i} k_1 \left[V - 1 \right] + k_2 \left[L_i - 1 \right] \right]$$

where the initial volume and initial lengths are unity and k_1 and k_2 are scalar parameters.

---

* This is the convention used in this report to indicate reference work. The first number is the reference number (found in Appendix F) and the second is the page number.

The extension modulus is not expected (predicted from molecular theory) to vary much with strain rate. Therefore, k_2 is reasonably assumed to be constant. The volume change effect is equivalent to the equation of state. This is somewhat dependent on the volume. The Los Alamos data will be used as an initial approximation for this relation. It has been experimentally observed that most materials are very nearly linear throughout their elastic range in extension, but not in compression.

So far, the theory has been elastic, i.e., no permanent deformations. Plastic (inelastic) effects are most naturally described in terms of strain and stress rates. It is believed that plastic phenomena arise largely from dislocation movement in the crystal structure. At normal temperatures most solids have an elastic region of strain and permanently deform when that range is exceeded. The transition point where the strain acquires a permanent component is called the yield point and is of great interest. At the yield point, the stress-strain law must be modified to account for plastic flow (permanent deformation).

The magnitudes of the side vectors $\vec{s}_i$ are

$$L_i = \overline{MAG} \circ \vec{s}_i = \sqrt{\vec{s}_i \cdot \vec{s}_i} = \sqrt{s_{\underline{ii}}}$$

If the absolute value of the difference in any pair of side vectors' magnitudes is greater than the yield level Y, the material is in a state of plastic flow. This is similar to the Tresca yield condition. The dependence of the stresses in plastic flow on the deformation rate can be formulated using the time rates of various measures of deformation.

A fundamental assumption in our work is that the a^i relating the stress tensor to the strain image tensor are given by functions of scalar tensor invariants. Some useful invariants are listed below.

$$\text{Volume} = V = \left| \vec{s}_i \cdot \vec{s}_j \right|^{1/2}$$

$$\text{Volume rate} = \frac{dV}{dt} \text{ (ordinary differentiation)}$$

Side lengths $= L_i = (s_{ii})^{1/2} = (\vec{s}_i \cdot \vec{s}_i)^{1/2}$

Side length rates $= \frac{dL_i}{dt}$ (ordinary differentiation)

Average of side lengths $= A = \frac{L_1 + L_2 + L_3}{3}$

Side length imbalance $= B_i = (L_i - A)^2$

This simplifies the mathematics considerably but retains the generality of more complicated formulations. Some of the expressions for a^i that we are now experimenting with are

$$a^i = \left[k_1 \left(\frac{1}{V} - 1\right) + k_2 \left(\frac{1}{L_i} - 1\right)\right] \frac{1}{L_i}$$

for the elastic range and

$$a^i = \left[k_1 \left(\frac{1}{V} - 1\right) + k_3 \frac{dB_i}{dt}\right] \frac{1}{L_i}$$

for the plastic range.

General, <u>simultaneous</u> elastic and plastic effects can only be described by the decomposition of the total strain into an elastic strain and a plastic strain. There are then two unknown strains, viz. any two of the plastic, elastic, and total strains. This is a vastly more complicated problem and will be undertaken later in the project.

2.3 Equations of Motion

The law of motion in invariant form is

$$\vec{F} = m\vec{A}$$

where $\vec{F}$ is the net force vector acting on mass m, and $\vec{A}$ is the acceleration vector.

For the present we assume that the spatial coordinates X^i are rectangular and coincident with the underlying reference $z_i\vec{I}$. In this case the original undeformed material cubes are parallel to the coordinate lines. Curvilinear spatial coordinates will be considered in later work.

The law of motion is simply

$$\frac{d}{dX^i}(\vec{M}_1 + \vec{M}_2 + \vec{M}_3) = \rho\frac{d^2\vec{P}}{dt^2}$$

where ρ is the density and $\vec{P}$ is the position vector expressed in the X^i.

3. DISCRETE VARIABLE MODEL

3.0 Introduction to the Computational Approach

A simple problem was chosen to facilitate the construction of the initial version of the computer code. One prism, traveling at one kilometer per second, collides with an identical prism which is at rest. It is assumed that there is no slippage of the surfaces at the interface.

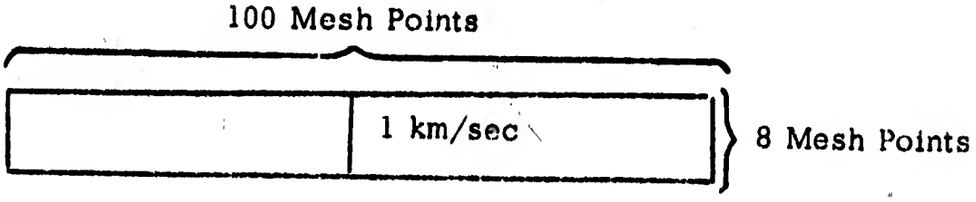

The discrete variable mesh is depicted below. The positions of the mass points are the mesh variables.

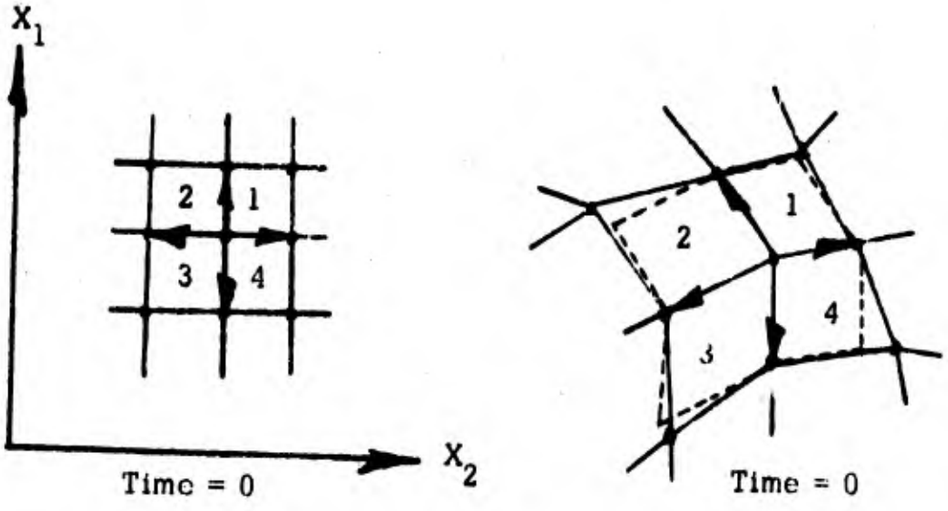

At each of the points there is a concentrated mass surrounded by four massless material squares. At time-zero each point P, has four unit vectors attached to it. These vectors are defined to be the unit length, directed line segments connecting P with its four nearest neighbors. As the points move (the material deforms) the vectors change length and orientation. The two vectors defining each of the four quadrants around P can be considered as undergoing a linear transformation from their initial (undeformed) to the deformed states.

Since the original two vectors are orthonormal, the transformation is just a matrix whose rows are just the components of two vectors after deformation. It can easily be shown that if the transformation matrix is denoted by A^I_J, then the nonlinear strain tensor e_{ij} is simply

$$e_{ij} = A^I_i \, A^I_j - \delta_{ij}$$

The components of the two side vectors are the components of the strain image tensor and are easily obtained from the tabulated mesh variables by a few subtractions. This makes calculation of the conventional nonlinear strain tensor trivial.

A^I_J is numerically identical to the strain image tensor. With the strain image tensor easily available, the stress tensor can be calculated from whatever stress-strain relation is being used. The four different states of deformation of the four material squares around P give rise to four forces which add to produce a resultant force at point P. The strain image tensor and its time derivative are used to calculate the stress vectors acting on the faces of each of the four parallelepipeds around point P. The stress-strain relations are the ones mentioned in Section 3.1.

The acceleration of point P is a simple calculation in these coordinates. An error vector at every point P is defined to be

$$\vec{E} = \vec{F} - m\vec{A}$$

where $\vec{E}$ = error vector

$\vec{A}$ = acceleration vector

$\vec{F}$ = net force vector

m = mass of point P.

Clearly at any given time point, the convergence criteria is that the length of the error vector at any point in the mesh is under some acceptable level.

Starting from time zero, a predictor routine uses the past velocities and accelerations to predict the positions of the mass (mesh) points at the next time position. There will be some error in the prediction. The corrector proceeds to systematically eliminate the error (reduce the error vectors to zero).

It can be shown that if all of the mass points are displaced from their predicted positions by a correction vector which is calculated from the error vectors and their derivatives, all the errors will simultaneously

decrease. The points are moved, the error vectors calculated again, and the process repeated until the error is reduced sufficiently. Then the prediction of the mass point positions is made for the next point in time. The corrector process is again used to converge to proper mass point positions from this time point.

3.1 Stress-Strain Relation

The relations we are presently using give the force vector across each face of the deformed parallelepiped (only two-dimensional in this problem) in terms of its side vectors (components of its strain image tensor).

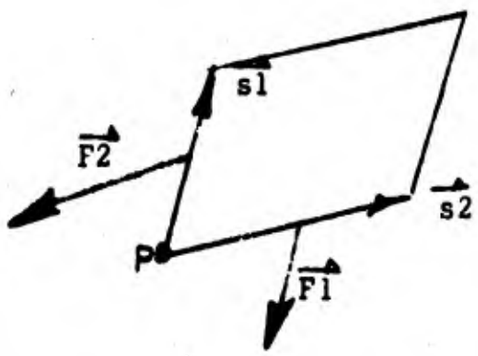

The side vectors $\vec{s1}$ and $\vec{s2}$ are shown in their positive directions and the force vectors are shown in their negative directions. $\vec{s1}$ and $\vec{s2}$ were originally orthonormal.

The force $\vec{F}$, acting on P as a result of the deformed material square shown is

$$\vec{F} = \frac{\vec{F1} + \vec{F2}}{2}$$

In the computer code, the following simple stress-strain rule is being used in order to be able to compare the numerical results with known work.

$$\vec{F2} = a_2 * \frac{\vec{s2}}{|\vec{s2}|}$$

$$\vec{F1} = a_1 * \frac{\vec{s1}}{|\vec{s1}|}$$

V = volume of parallelepiped

where

$$a_1 = -k_1 * (|\vec{s1}| - 1) - k_2 * (V - 1) + k_3 * \frac{d}{dt} |\vec{s1}|$$

$$a_2 = -k_1 * (|\vec{s2}| - 1) - k_2 * (V - 1) + k_3 * \frac{d}{dt} |\vec{s2}|$$

k_1 and k_2 are the classical Lame's constants. k_3 is arbitrarily at the present time. We have done some experimenting with different values of k_3 and have found that it affects the results dramatically.

Various nonlinear and rate dependent rules (extensions of Section 2.2) are being programmed for computer analysis, but we do not have the numerical results at this time.

3.2 Boundary Conditions

Because the forces from each material square are calculated independently of the others, the boundary conditions are trivial. A control number is recorded at each material square and indicates, among other things, the type of material in that square.

For example,

Symmetry Line

V	V	V	V	Al	Al	Al
V	V	V	V	Al	Al	Al
V	V	V	V	Al	Al	Al
V	V	V	V	Al	Al	Al
Fe	Fe	Fe	Fe	Fe	Fe	Fe
Fe	Fe	Fe	Fe	Fe	Fe	Fe
Gl	Gl	Gl	Gl	Gl	Gl	Gl

where V denotes vacuum
Al denotes aluminum
Fe denotes steel
Gl denotes glass

In this way the boundary conditions take care of themselves.

Curved boundaries may be approximated by jagged rectangular boundaries or by a more sophisticated scheme like interpolation, etc. If the number of mesh points is reasonably large, jagged rectangular boundaries may be reasonable approximations.

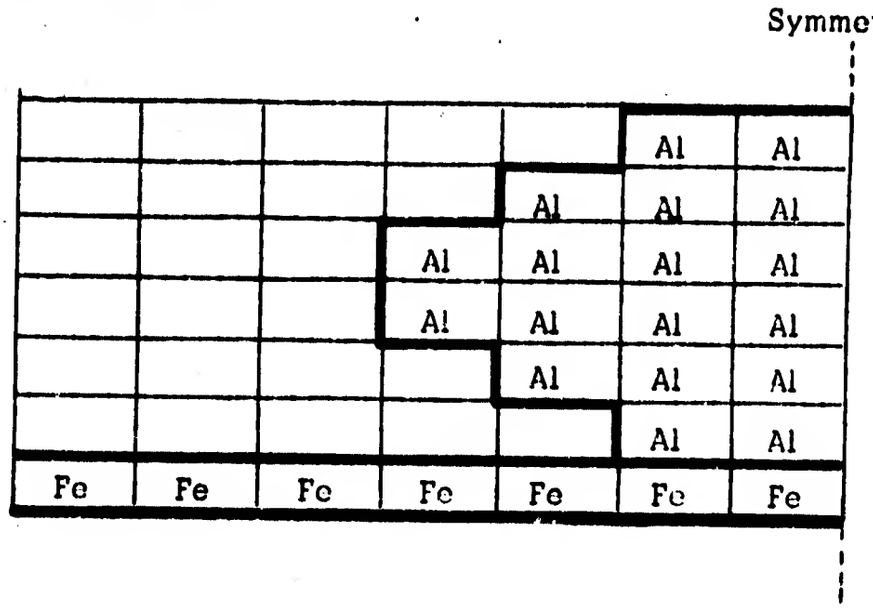

4. RESULTS AND CONCLUSIONS

4.0 Preliminary Numerical Results

The problem we have used in developing the computer code is the end-on impact of two identical prisms having a relative velocity of 1 km/sec. The material was aluminum and the standard values of the static elastic constants were used in a linear elastic relation. Rate dependence (as a sort of viscosity) was added and was varied from none to dependence on second time derivatives.

It should be emphasized that these results are preliminary and are presented as evidence of the feasibility of the general numerical method. Thus far, we have not critically compared these results with other work in the field. The detailed examination of the spectrum of likely stress-strain rules is also just beginning.

The graphical display in Figures 4.1-1, 4.1-2 and 4.1-3 shows the mesh and samplings of the velocity field at times shortly after impact. The displacements are still small. These calculations took about ten minutes on an IBM-7040. Output was generated only every five time points.

The rate of propagation of the displacement wave is about 5 km/sec, which agrees with the measured speed of sound in aluminum (7,1863). As deduced from Riney's work, the shape of the velocity profile is about as it should be for a strongly rate-dependent stress-strain rule (8,32). The rule used in these computations was

$$\vec{F}_i = a^i \vec{s}_i$$

$$a^i = \frac{1}{L_i}\left[k_1 (V - 1) + k_2 (L_i - 1) + k_3 \left(\frac{d^2 L_i}{dt^2}\right)\right]$$

where $\vec{F}_i$ is the stress vector through side i. See section 2.2 for notation and details.

The basic numerical method is applicable to more interesting models. In the next phase of our work we will consider, among other things, cylindrical geometries, nonlinear elastic rules and simultaneous elastic and plastic stresses.

As soon as we optimize the computer code and decide upon a stress-strain rule, we will make long-time runs to observe large plastic deformations.

INITIAL CONFIGURATION

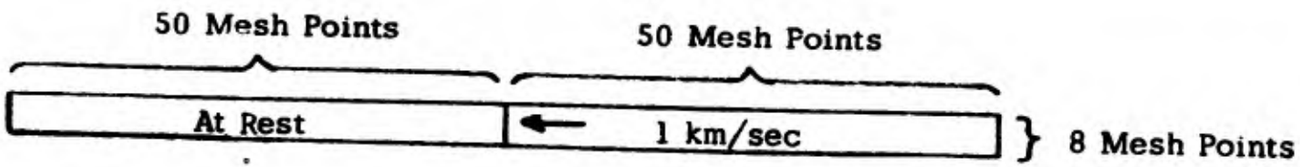

FIGURE 4.1-1

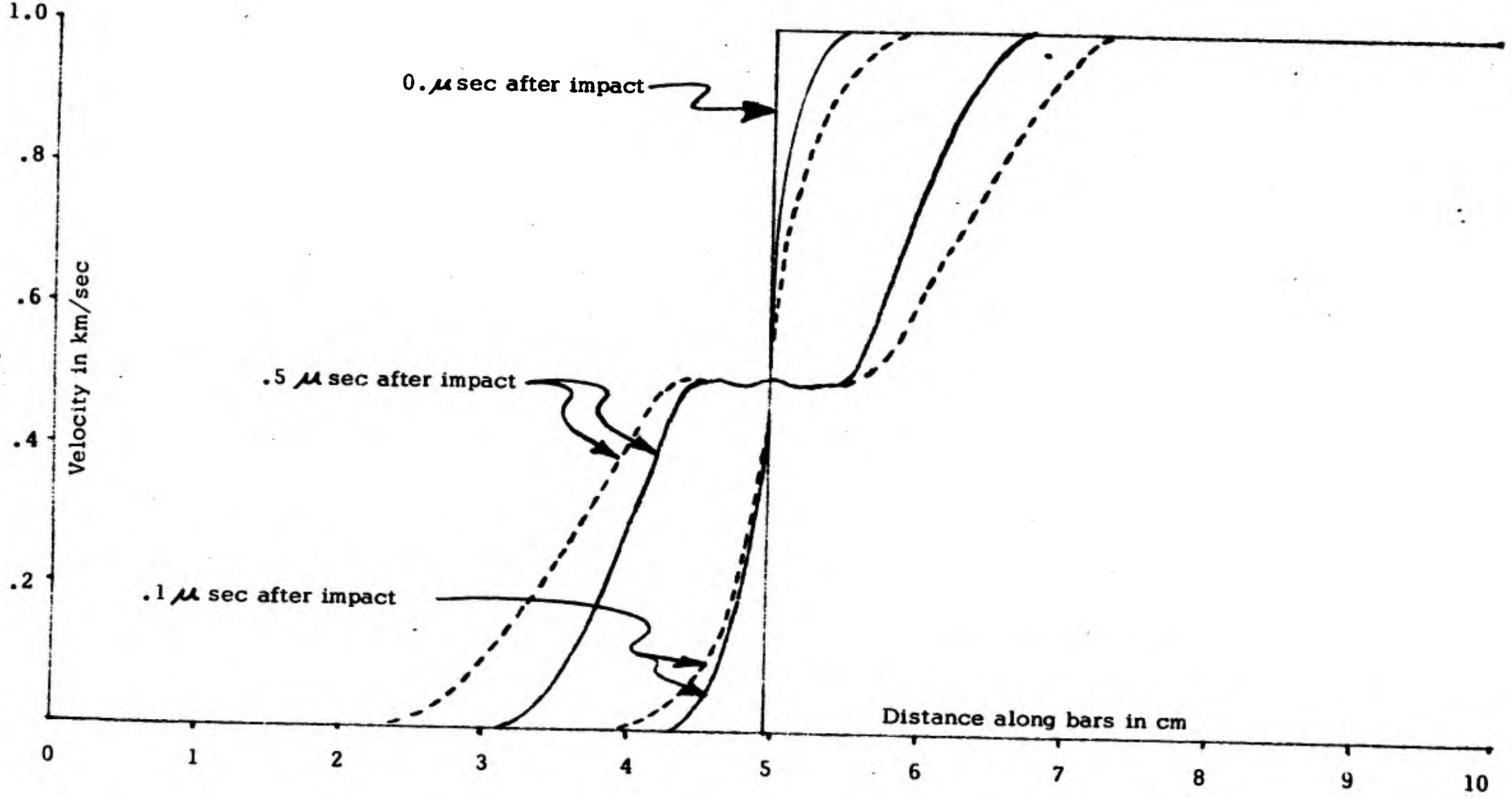

FIGURE 4.1-2

Longitudinal component of the velocity profile along the bars.
Dotted lines are profiles at the center.
Solid lines are profiles at the surface.

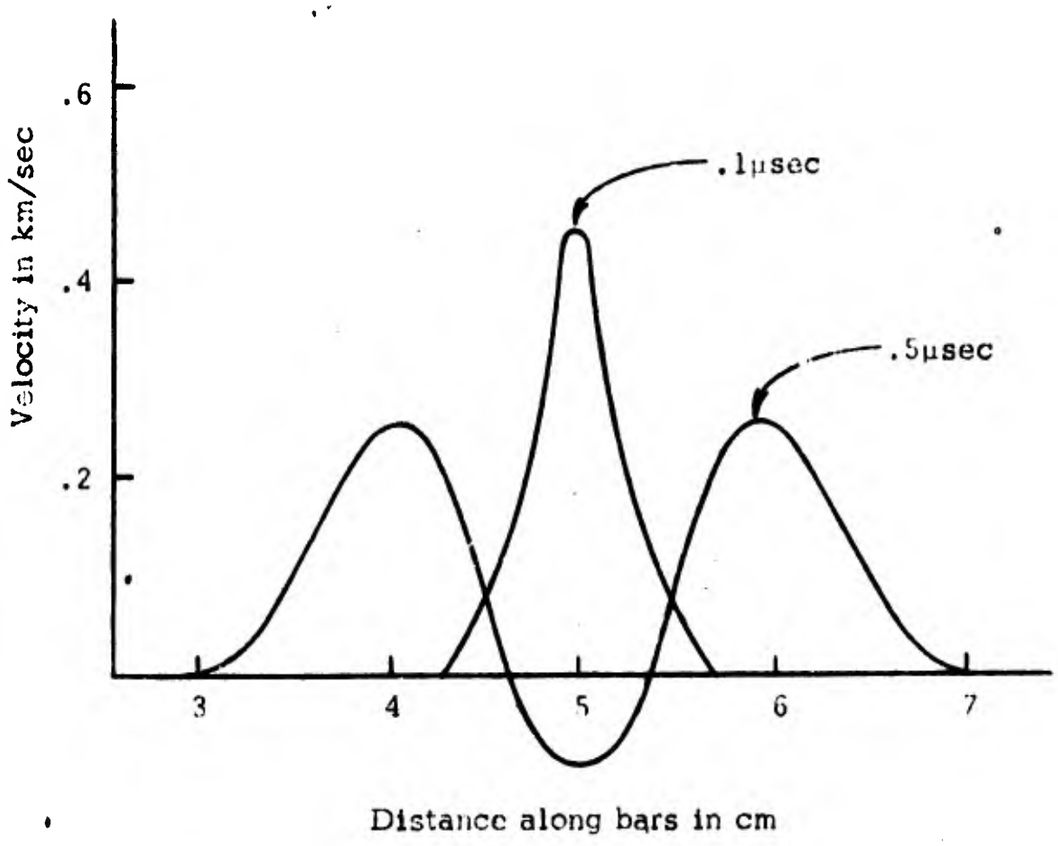

Profile of Transverse Component of Velocity at Surface of Bars

FIGURE 4.1-3

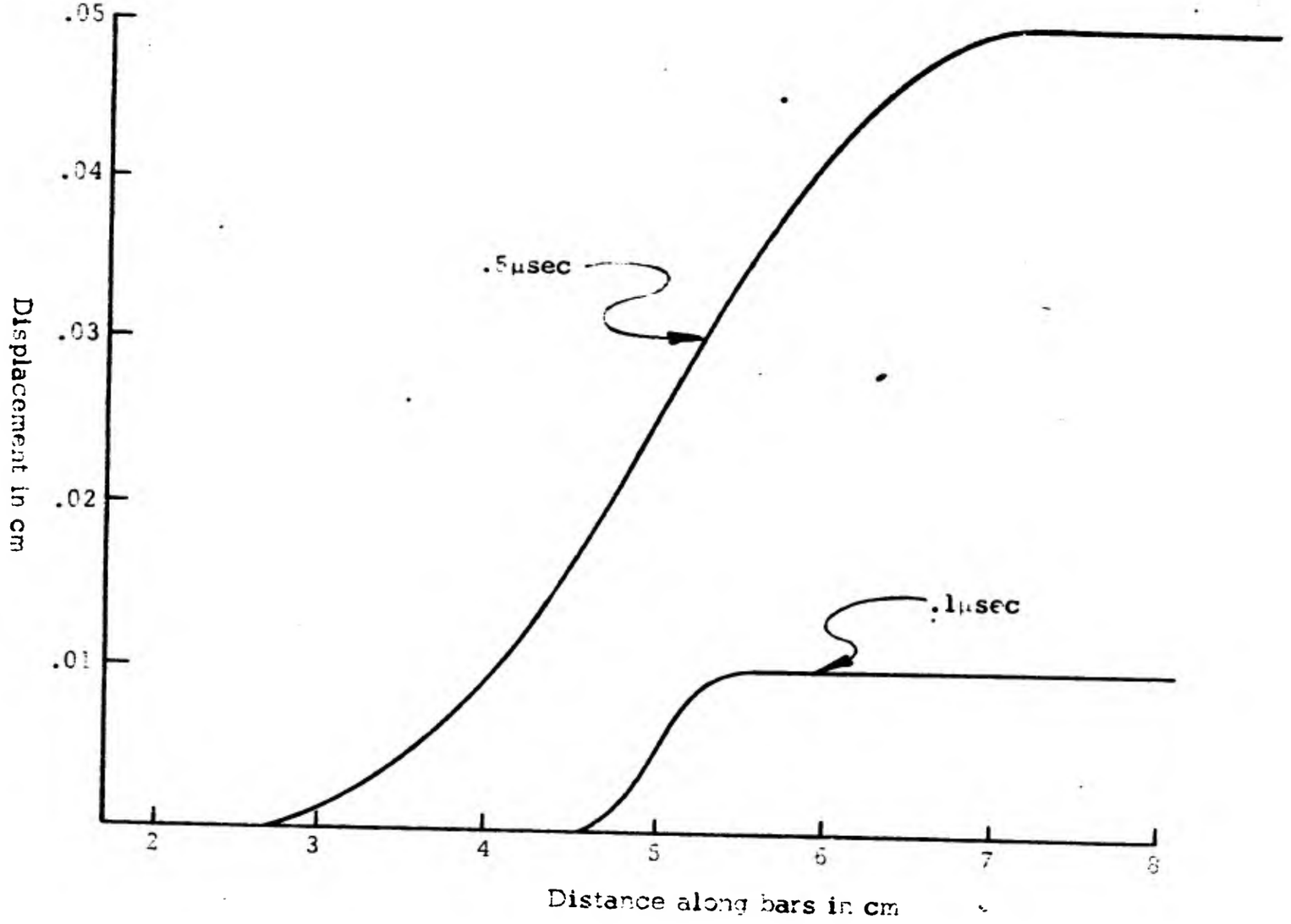

Longitudinal Displacement Profile Down the Center of the Bars

FIGURE 4.1-4

APPENDICES

APPENDIX A: OUTLINE OF NOTATION

A.1 Variable Symbols

1. A variable may be represented by a simple variable symbol such as

   $$a, x, y, r, \alpha \quad \text{etc.}$$

   or a compound variable symbol such as

   $$\overline{X11C2}, \quad \overline{BAT}, \quad \overline{DOT}, \quad \overline{HEAT}$$

   A compound variable symbol must start with a letter and be tied together with a bar.

2. Indices which are not of tensor nature may be included in parentheses within a compound variable symbol.

   $$\overline{X1(I,J)}, \quad \overline{BAT(1,K)}, \quad \text{etc.}$$

3. When discussing transformations, variables beginning with upper case letters refer to the initial space and variables beginning with lower case letters refer to the space after transformation.

4. A variable symbol with subscript or superscript indices represents a set of quantities. An arrow over the variable symbol indicates that each of the elements is a tensor.

Example

Consider a vector (a first order tensor) in three space.

$$\vec{V} = V^k \vec{e}_k$$

Note

$\vec{V}$ is a tensor

$\vec{e}_k$ is a set of 3 tensors which form a basis in which $\vec{V}$ can be expressed.

V^k are the components of the tensor referred to the basis $\vec{e}_k$.

A.2 Rules for Indexed Variables

1. Indices appear as subscripts or superscripts or within the variable symbol.
2. When a variable is a tensor, the subscripts refer to covariant components and superscripts refer to contravariant components.
3. When discussing transformations, upper case indices usually are used to refer to initial coordinates and lower case indices to refer to the transformed coordinates.
4. When an index appears more than once in a product, that index is summed over its range.
5. A bar under an index suspends the summation convention on that index only for that variable.

6. A bar over an index means that the index is not a tensor index.

7. Parentheses around a tensor index mean that the index refers to the physical components of the tensor.

8. Exponents on a variable are always superscripts. Whenever there is a possibility of confusion, the exponent is put in brackets or parentheses.

Example

$$\overline{XX}^{I}_{J}\,[2X+1] \equiv (\overline{XX}^{I}_{J})^{2X+1}$$

A..3 Operation Symbols

1.	Summation	$\sum$
2.	Determinant	$\lvert\ \rvert$
3.	Scalar Multiplication of A and B	A*B or AB
4.	Addition	+
5.	Subtraction	-
6.	A divided by B	$\frac{A}{B}$ or A/B
7.	Absolute Value	$\lVert\ \rVert$ or $\overline{ABS}$.
8.	Integral	$\int$
9.	Operator "f" acting on argument "X"	f ∘ X or f ∘ (X)
10.	Ordering of operations uses parentheses and brackets	( ) [ ]

11. Inner or dot product of two vectors $\vec{A} \cdot \vec{B}$

12. Cross product of two vectors $\vec{A} \times \vec{B}$

13. Tensor product of two tensors $\vec{A} \otimes \vec{B}$

14. Magnitude or modulus of a vector $\overline{MAG}\bullet$ or MOD•

A.4 Common Operators

1. The very commonly used functional operators such as trig functions, etc., are not required to have the operation symbol.

Example

$$\sin \Theta \equiv \overline{\sin} \circ \Theta$$

2. $\frac{dX}{dY}$ is the partial of X with respect to Y.

3. A comma may be used to indicate ordinary partial differentiation.

$$\frac{dY^i}{dX^j} = Y^i{}_{,j} \quad \text{and} \quad \frac{dY_i}{dX^j} = Y_{i,j}$$

4. A ∇ is used to indicate the covariant or absolute differential of a quantity.

Example

The absolute differential of a tensor $\vec{X}$ with respect to Y^j is

$$\overrightarrow{\nabla X}_{,j} = \frac{\nabla \vec{X}}{dY^j}$$

5. A semicolon is used to indicate covariant or absolute differentiation of tensor components.

Example

$$Y^i{}_{;j} \text{ and } Y_{i;ji} \text{ etc.}$$

A.5 Special Symbols

1. The generalized Kroneker delta is defined as

$$\delta^{mn\ldots pq}_{ij\ldots kl} = \begin{cases} 0 \text{ when the indices are all numerically equal} \\ 1 \text{ otherwise} \end{cases}$$

2. The permutation symbol is defined as

$$E_{ij\ldots kl} = \begin{cases} 1 & \text{for even permutations of the indices} \\ -1 & \text{for odd permutations} \\ 0 & \text{otherwise} \end{cases}$$

APPENDIX B: SOME DEFINITIONS CONCERNING VECTOR AND TENSOR SPACES OVER THE FIELD OF REAL NUMBERS

B.1 Scalar Multiplication in a Vector Space

The vector $\vec{X}$ is an undefined abstract quantity. Multiplying a vector $\vec{X}$, by a real number, b, is written (5,1)

$$b*\vec{X} \text{ or simply } b\vec{X}$$

The asterisk is used when there may be confusion with other product and functional notations.

1. $1*\vec{X} = \vec{X}$
2. $a*\vec{X}+b*\vec{Y} = b*\vec{Y}+a*\vec{X}$
3. $a*(b*\vec{X}) = (a*b)*\vec{X}$
4. $(a+b)*\vec{X} = a*\vec{X}+b*\vec{X}$
5. $a*(\vec{X}+\vec{Y}) = a*\vec{X}+a*\vec{Y}$
6. $\vec{X}+\vec{Y}$ is undefined

B.2 Vector Spaces

Any n distinct vectors $\vec{X}_i$ may be used to generate a vector space. The space is the collection of all possible $a^i \vec{X}_i$ where the a^i are selected from the real numbers. The $a^i \vec{X}_i$ are also called vectors. Since there are n vectors used in the linear form, $a^i \vec{X}_i$, the space generated is said to be n-dimensional.

A general vector in the space may be symbolized $\vec{V} = a^i \vec{X}_i$. The $\vec{X}_i$ are called the basis or generator vectors (or just the basis) of the space because all the vectors in the space are linear combinations of $\vec{X}_i$. The a^i are called the components of the vector $\vec{V} = a^i \vec{X}_i$.

B.3 Vector Addition

Referred to a basis, the addition of two arbitrary vectors in the space has the following meaning. If $\vec{V} = a^i \vec{X}_i$ and $\vec{W} = b^i \vec{X}_i$, the rules defining scalar combinations of vectors may be used to express the otherwise undefined sum of two vectors.

$$\vec{V} + \vec{W} = a^i \vec{X}_i + b^i \vec{X}_i$$

$$\vec{V} + \vec{W} = (a^i + b^i) \vec{X}_i$$

B.4 Vector Products

The addition of two different basis vectors is undefined except in terms of components relative to some other basis. However, several products of basis vectors are defined in terms of their properties.

B.5 Dot Product

The dot product of a pair of vectors is a scalar.

$$\vec{V} \cdot \vec{W} = \vec{V} \cdot \vec{W} = \text{some scalar}$$

$$(a\vec{V}) \cdot \vec{W} = a\,(\vec{V} \cdot \vec{W}) = \vec{V} \cdot (a\vec{W})$$

$$a(\vec{V} + \vec{W}) = a\vec{V} + a\vec{W}$$

The array of all the possible dot products of the basis vectors is

$$g_{ij} = \vec{X}_i \cdot \vec{X}_j = \text{array of scalars}$$

$$g_{ij} = g_{ji}$$

The symmetric array g_{ij} defines the numerical values of the dot products of the basis vectors and therefore all the vectors in the space.

$$\left(a^i \vec{X}_i\right) \cdot \left(b^j \vec{X}_j\right) = a^i b^j \left(\vec{X}_i \cdot \vec{X}_j\right) = a^i b^j g_{ij}$$

B.6 Tensor Products

The tensor product of two vectors is indicated

$$\vec{V} \otimes \vec{W}$$

and is in itself an undefined object. It is a tensor of rank two, being constructed from two tensors of rank one, namely vectors. Any number of vectors may form a tensor product. The tensor product of n vectors is a tensor of order n. All tensors are labeled with arrows over their symbol.

$$\vec{A} = \vec{B} \otimes \vec{C} \otimes \vec{D} \otimes \vec{E}$$

A is a fourth order tensor. Usually A has indices indicating its order, but in the instances where it does not, a number that indicates the order may be put over the arrow to avoid confusion.

$$\vec{A} = \vec{B} \otimes \vec{C} \otimes \vec{D} \otimes \vec{E}$$

The rules defining the tensor product are

1. $\vec{A} \otimes \vec{B} \neq \vec{B} \otimes \vec{A}$, in general
2. $\vec{A} \otimes (\vec{B} + \vec{C}) = \vec{A} \otimes \vec{B} + \vec{A} \otimes \vec{C}$

   $(\vec{B} + \vec{C}) \otimes \vec{A} = \vec{B} \otimes \vec{A} + \vec{C} \otimes \vec{A}$
3. $a * (\vec{B} \otimes \vec{C}) = (a * \vec{B}) \otimes \vec{C} = \vec{B} \otimes (a * \vec{C})$

As every vector is referred to a basis, likewise all second order tensors may be referred to a tensor basis of the form

$$\vec{X}_{ij} = \vec{X}_i \otimes \vec{X}_j$$

where $\vec{X}_i$ is a vector basis.

In general,

$$\vec{X}_{ijk \ldots z} = \vec{X}_i \otimes \vec{X}_j \otimes \vec{X}_j \otimes \ldots \otimes \vec{X}_z$$

B.7 Relation of the Dot and Tensor Products

$$\vec{V} \cdot (\vec{X} \otimes \vec{Y}) = (\vec{V} \cdot \vec{X}) * \vec{Y}$$

$$(\vec{X} \otimes \vec{Y}) \cdot \vec{V} = \vec{X} * (\vec{Y} \cdot \vec{V})$$

$$\vec{V} \cdot (\vec{X} \otimes \vec{Y} + \vec{Z} \otimes \vec{W}) = \vec{V} \cdot (\vec{X} \otimes \vec{Y}) + \vec{V} \cdot (\vec{Z} \otimes \vec{W})$$

In general,

$$\vec{V} \cdot (\vec{X} \otimes \vec{Y}) \neq \vec{X} * (\vec{V} \cdot \vec{Y})$$

B.8 Covariant and Contravariant Bases

The set of vectors $\vec{e}_i$ is a basis for an n-dimensional vector space. The subscript i indicates that they were arbitrarily chosen to be called a covariant basis. Vectors referred to a covariant basis have contravariant components, x^i. The index being in the superscript position indicates contravariant character.

For every covariant basis $\vec{e}_i$ there is a reciprocal contravariant basis $\vec{e}^i$ defined by

$$\vec{e}_i \cdot \vec{e}^j = \delta_i^{\ j}$$

This relation implicitly defines the reciprocal basis. Given a basis $\vec{e}_i$ it is a routine calculation to find the transformation, connecting $\vec{e}_i$ with $\vec{e}^i$.

$$\vec{e}^i = g^{ij} \vec{e}_j$$

The inverse transformation is g_{ij}. The g_{ij} and g^{ij} are the metrics of the $\vec{e}_i$ and $\vec{e}^j$ bases respectively.

B.9 Products of Covariant and Contravariant Vectors

The dot product rules are summarized below.

$$\vec{e}^i \cdot \vec{e}_j = \delta^i_{\ j}$$

$$\vec{e}^i \cdot \vec{e}^j = g^{ij}$$

$$\vec{e}_i \cdot \vec{e}_j = g_{ij}$$

Tensor products of covariant and contravariant vectors are called mixed tensors. For example,

$$\vec{e}_i \otimes \vec{e}^j \otimes \vec{e}_k = \vec{c}_i{}^j{}_k$$

The component representations of tensors in this basis are written

$$\vec{T} = t^{i\ k}_{j}\ \vec{e}_{i\ k}^{\ j}$$

B.10 Contracted Tensor Products

There are three possible dot products of the two tensors $(\vec{A} \otimes \vec{B} \otimes \vec{C})$ and $\vec{D}$.

$$(\vec{A} \cdot \vec{D}) * \vec{B} \otimes \vec{C}$$

$$(\vec{B} \cdot \vec{D}) * \vec{A} \otimes \vec{C}$$

$$(\vec{C} \cdot \vec{D}) * \vec{A} \otimes \vec{B}$$

These products are tensors of one lower order. In general, they are not identical, so that a particular product must be specified. The tensor $\vec{A} \otimes \vec{B} \otimes \vec{C} \otimes \vec{D}$ can be contracted by replacing one or more of the tensor products by dot products. For example,

$$(\vec{A} \cdot \vec{B}) * \vec{C} \otimes \vec{D}$$

$$(\vec{A} \cdot \vec{B}) * (\vec{C} \cdot \vec{D})$$

$$(\vec{A} \otimes \vec{D}) * (\vec{B} \cdot \vec{C})$$

Usually the factors of the products will have indices. When indicating the dot product of two tensor bases, the following convention is useful.

$$\vec{A}_i{}^j{}_k \equiv \vec{g}_i \otimes \vec{g}^j \otimes \vec{G}_k$$

$$\vec{B}_{nm} \equiv \vec{G}_n \otimes \vec{g}_m$$

$$(\vec{A}_i{}^j{}_k) \cdot (\underset{\equiv\equiv}{\vec{B}}_{ik}) \equiv (\vec{g}_i \cdot \vec{G}_n) * \vec{g}^j * (\vec{G}_k \cdot \vec{g}_m)$$

B.11 Permutation Symbol

The permutation symbol is used in building determinants. It is defined as (6, 85)

$$E^{ijk} = 1 \text{ for even permutation of } (i,j,k)$$
$$= -1 \text{ for odd permutation of } (i,j,k)$$
$$= 0 \text{ otherwise}$$

This definition is extended to more or fewer indices.

B.12 Volume Tensor

In some preferred basis $\vec{e}_i$ (usually, but not necessarily, one for which $\vec{e}_i \cdot \vec{e}_j = \delta_{ij}$), the volume tensor is defined as

$$\vec{V} = E^{ijkn} \vec{e}_i \otimes \vec{e}_j \otimes \vec{e}_k \otimes \vec{e}_n$$

Where E^{ijkn} is the permutation symbol.
Now the components in all other bases are defined by the rules of tensor transformation. In other than the preferred basis, the volume tensor components are written V^{ijkn} to avoid confusion with the permutation symbol E^{ijkn} (which is not the components of a tensor).

APPENDIX C: COORDINATE SYSTEMS

In discussing deformation, it is very important to accurately define the various coordinate systems used and their interrelationships.

C.1 General Coordinates in Terms of an Underlying Vector Space

All coordinate systems are defined in terms of an underlying real Euclidean vector space generated by an orthonormal basis $\vec{I}_i$. The points in some derived coordinate manifold X^i, may be associated (usually) in a one-to-one correspondence with the points described by the general position vector $\vec{P}$, in the underlying Euclidean vector space. If the position vector is $\vec{P} = z^i \vec{I}_i$, the correspondence may be symbolized

$$X^i \longleftrightarrow \vec{P} \equiv z^j \vec{I}_j$$

or, in terms of components of P

$$X^i = f^i \circ (z^j)$$

and inversely $$z^i = F^i \circ (X^j)$$

The metric of the underlying vector space is δ_{ij}, i.e. $\vec{I}_i \cdot \vec{I}_j = \delta_{ij}$. The local metric of the X^i coordinates may be defined by the relation to the underlying space. A local vector space with basis $\vec{G}_j$ may be attached to every point X^i in the derived coordinates, by the following definition:

$$\vec{G}_j = \frac{dz^i}{dX^j} \vec{I}_i$$

From this, the local metric at X^i is defined as

$$G_{ij} = \vec{G}_i \cdot \vec{G}_j = \frac{dz^k}{dX^i} \frac{dz^m}{dX^j} \vec{I}_k \cdot \vec{I}_m$$

$$G_{ij} = \frac{dz^k}{dX^i} \frac{dz^k}{dX^j}$$

C.2 Coordinates Used in Deformation Theory

A geometrical point described by the tip of the position vector $\vec{P}$ of the underlying space may be specified by giving the components of $\vec{P}$. The components of $\vec{P}$ relative to the orthonormal basis $\vec{I}_i$ are z^i and can be thought of as coordinates. Other derived coordinates are ultimately defined relative to the z^i.

The two most important derived coordinate systems are the material coordinates and the spatial coordinates. The material coordinates are used to label the material points and usually do not change with time. The spatial coordinates are used to describe the position of each material point and usually do not change with time either. The exact geometrical state of deformation of a material body is described by the functional relation of each of its material points to spatial points. This defines the spatial positions of the material points of all items. In this report, the spatial coordinates are symbolized X^i, and the material coordinates are x^i.

For convenience in notation, time will be included with the spatial coordinates to make a four dimensional manifold. Time in the underlying space is represented by $z^4 \vec{I}_4$. The material and spatial coordinates are chosen at time zero and usually are not changed thereafter. The spatial coordinates may be defined by

$$\left.\begin{aligned} z^i &= S^i \circ (X^j) \\ \text{and inversely} \quad X^i &= s^i \circ (z^j) \end{aligned}\right\} \quad \text{for } i \text{ and } j = 1 \rightarrow 3$$

$$\text{and} \quad X^4 = z^4$$

The material coordinates may be defined by

$$\left.\begin{aligned} z^i &= M^i \circ (x^j) \\ \text{and inversely} \quad x^i &= m^i \circ (z^j) \end{aligned}\right\} \quad \text{for } i \text{ and } j = 1 \rightarrow 3$$

$$\text{and} \quad x^4 = z^4$$

These definitions are usually made so that at time $= z^4 = 0$ the $x^i = X^i$ numerically.

The deformation of a material is described by the relation of the x^i to the X^i at later times.

$$\left.\begin{aligned} X^i &= F^i \circ (x^j) \\ \text{and inversely} \quad x^i &= f^i \circ (X^j) \end{aligned}\right\} \left\{\begin{aligned} j &= 1 \quad 4 \\ i &= 1 \quad 3 \end{aligned}\right.$$

$$\text{and} \quad X^4 = x^4 = z^4$$

APPENDIX D: COVARIANT DIFFERENTIATION

We shall define covariant or absolute differentiation of a tensor with respect to some path S as the ordinary differentiation of the tensor along the path when both (tensor and path) are expressed in the underlying coordinate space $z^i \vec{I}_i$. Absolute differentiation is indicated in vector form independent of coordinates. For example, the derivative of the second order tensor $\vec{T}$ with respect to the displacement vector $\vec{dP}$ is written $\vec{dT}/\vec{dP}$. Since the tensor and path are usually described in some other coordinates, formulae must be derived for covariant differentiation with respect to arbitrary metrics.

To properly derive these formulae, the tensor product of two vector spaces should be reviewed (5,29). The tensor basis $\vec{G}_{IK}$ derived from an arbitrary vector basis $\vec{G}_I$ is $\vec{G}_{IK} = \vec{G}_I \otimes \vec{G}_K$ where $\otimes$ indicates the tensor product.* Just as all vectors in the vector space may be referred to $\vec{G}_K$, all second order tensors in the vector space may be referred to $\vec{G}_{IK}$. The covariant derivative is a tensor of one higher order than $\vec{T}$.

In general curvilinear coordinates given by

$$z^I = z^I (x^k)$$

or $$x^k = x^k (z^I)$$

---

* The properties of the tensor product are almost the same as the dot product. $\vec{X} \otimes (\vec{Y} + \vec{Z}) = \vec{Y} \otimes \vec{Y} + \vec{X} \otimes \vec{Z}$ and $b\,\vec{X} \otimes \vec{Y} = \vec{X} \otimes b\vec{Y} = b\,(\vec{X} \otimes \vec{Y})$ and $\vec{X} \otimes (\vec{Y} \otimes \vec{Z}) = (\vec{X} \otimes \vec{Y}) \otimes \vec{Z}$. However, in general $\vec{X} \otimes \vec{Y} \neq \vec{Y} \otimes \vec{X}$

The second order tensor $\vec{\vec{T}}$ has the representation

$$\vec{\vec{T}} = t^{ij} \vec{\vec{g}}_{ij}$$

and $\vec{dP}$ becomes $dx^i \vec{g}_i$

where $\vec{\vec{g}}_{ij}$ is the new local tensor basis.

Covariant differentiation with respect to particular coordinates is indicated by a semicolon. Covariant differentiation not referred to a particular basis is indicated by .

$$\vec{\nabla T} = \frac{d\vec{T}}{d\vec{P}} = \frac{d}{d\vec{P}} \left[t^{ij} \vec{\vec{g}}_{ij} \right]$$

$$\vec{\nabla T} = \frac{d}{dx^i} \left[t^{ij} \vec{\vec{g}}_{ij} \right] \otimes \vec{g}_k = t^{ij}{}_{;k} \vec{\vec{g}}_{ijk}$$

where $\vec{\vec{g}}_{ijk} = \vec{g}_i \otimes \vec{g}_j \otimes \vec{g}_k$

The $\vec{\vec{g}}_{ij}$ are now functions of the coordinates and must be differentiated along with the tensor components.

$$\frac{d}{dx^k} \left[t^{ij} g_{ij} \right] \otimes \vec{g}_k = \left[\frac{dt^{ij}}{dx^k} + \frac{d\vec{\vec{g}}_{ij}}{dx^k} \right] \otimes g_k$$

$$\frac{d}{dx^k} \left[t^{ij} g_{ij} \right] \otimes \vec{g}_k = \left[\frac{dt^{ij}}{dx^k} \vec{\vec{g}}_{ij} + t^{ij} \frac{d\vec{\vec{g}}_{ij}}{dx^k} \right] \otimes \vec{g}_k$$

where

$$\frac{d\vec{\vec{g}}_{ij}}{dx^k} = \frac{d}{dx^k} \left[\vec{g}_i \otimes \vec{g}_j \right]$$

$$\frac{d\vec{\vec{g}}_{ij}}{dx^k} = \frac{d\vec{g}_i}{dx^k} \otimes \vec{g}_j + \vec{g}_i \otimes \frac{d\vec{g}_j}{dx^k}$$

Now $\frac{d\vec{g}_i}{dx^k}$ must be found.

$$\vec{g}_i = \frac{dz^I}{dx^i}\,\vec{I}_I \equiv z^I{}_{,i}\,\vec{I}_I$$

and

$$\vec{I}_I = \frac{dx^i}{dz^I}\,\vec{g}_i \equiv x^n{}_{,I}\,\vec{g}_n$$

Therefore

$$\frac{d\vec{g}_i}{dx^k} = \frac{d^2 z^I}{dx^k\, dx^i}\,\vec{I}_I$$

$$\frac{d\vec{g}_i}{dx^k} = \left(\frac{d^2 z^I}{dx^k\, dx^i}\right)\frac{dx^n}{dz^I}\,g_n \equiv \begin{matrix} n \\ k\ \ i \end{matrix}\,\vec{g}_n$$

The Christoffel symbols of the second kind are defined and symbolized as follows:

$$\left\{\begin{matrix} n \\ k\ \ i \end{matrix}\right\} = \left(\frac{d^2 z^I}{dx^k\, dx^i}\right)\ \frac{dx^n}{dz^I}$$

Using this notation, the covariant differentiation becomes much more compact.

$$\frac{d\vec{g}_{ij}}{dx^k} = \left\{\begin{matrix} n \\ k\ \ i \end{matrix}\right\}\vec{g}_n \otimes \vec{g}_j + \left\{\begin{matrix} n \\ k\ \ j \end{matrix}\right\}\vec{g}_i \otimes \vec{g}_n$$

Substituting we obtain

$$\frac{d}{dx^k}\left[t^{ij}\,\vec{g}_{ij}\right] \otimes \vec{g}_k = \left[t^{ij}{}_{;k}\,\vec{g}_{ij} + t^{ij}\left\{\begin{matrix} n \\ k\ \ i \end{matrix}\right\}\vec{g}_{nj} + t^{ij}\left\{\begin{matrix} n \\ k\ \ j \end{matrix}\right\}\vec{g}_{in}\right] \otimes \vec{g}_k$$

$$\vec{\nabla} T = t^{ij}_{;k} \vec{g}_{ijk} = t^{ij}_{;k} \vec{g}_{ijk} + \left\{ \begin{matrix} i \\ k \quad n \end{matrix} \right\} nj \vec{g}_{ijk} + \left\{ \begin{matrix} j \\ k \quad n \end{matrix} \right\} t^{in} \vec{g}_{ijk}$$

and finally, $$\vec{\nabla} T = \left(t^{ij}_{,k} + \left\{ \begin{matrix} i \\ k \quad n \end{matrix} \right\} t^{nj} + \left\{ \begin{matrix} j \\ k \quad n \end{matrix} \right\} t^{in} \right) \vec{g}_{ijk}$$

APPENDIX E: A NUMERICAL METHOD FOR THE SOLUTION OF SOME PARTIAL DIFFERENTIAL EQUATIONS

E.1 Introduction

The purpose of this section is to present a numerical procedure for solving finite difference approximations of some systems of nonlinear partial differential equations.

To illustrate the scheme, we shall discuss an example involving a two-dimensional, rectangular, finite difference mesh. Several variables are tabulated at each of the mesh points. At every mesh point there is defined one difference equation for each dependent variable (at that mesh point).

The exact form of the difference equations will depend on the original differential equations, the boundary conditions, and the type of difference approximations used.

This method requires that the system of difference equations have an exact solution with some specific properties. This poses no difficulty in most physically oriented problems.

A special scalar parameter k, is introduced in the differential, and hence the difference equations. The difference equations are then written in homogeneous form $f_m = 0$, so that a point residual R_m may be defined as the sum of the squares of the difference functions at the point. The index m enumerates all of the mesh points. A system residual S, is defined as the sum of all the equation residuals. Since the system residual is necessarily positive, the solution of the system may be reached by minimizing S as a function of all the dependent variables throughout the mesh. Because the difference equations are loosely connected, minimization using a variation of Newton's method in many variables is computationally feasible. Stability is not a problem with this technique, but in complicated, highly nonlinear problems, computational time and memory requirements may become excessive.

We have developed a computer code (IBM-7040/FORTRAN IV) for the solution of a formidable set of equations describing a two-dimensional high velocity impact of elasto-plastic materials. Our numerical experience with this problem will be discussed later.

E.2 Notation and Parameterization of the Equations

The original system of differential equations and boundary conditions must be rewritten to include a special scalar parameter, k. At some value of the parameter, the equations must be identical with the original equations. At another value of the parameter, the equations must degenerate to a form with a known solution. Also, at every intermediate value of the parameter, say k = c, the corresponding solution W_c and the solutions W_k for neighboring values of k must be such that

$$\text{limit } (W_k) = W_c$$
$$k \longrightarrow c$$

As a very simple example, consider Poisson's equation in two independent variables, x and y.

$$\nabla^2 \circ V = g \circ (x, y)$$

and

$$V = h \circ \left[x \circ (s),\ y \circ (s) \right] = h \circ (s) \text{ over the boundary } s.$$

Possible choices for the parameterized equations are

$$\nabla^2 \circ V = K * g \circ (x,y)$$

and

$$V = k * h \circ (s)$$

Clearly there is a known solution for k = 0, viz. V = 0, and the desired equations are duplicated when k = 1. From physical considerations it is plausible that solutions exist for all $0 \leqslant k \leqslant 1$. When the differential equations are converted to the difference approximations, k will appear in a similar role in the difference equations.

$\nabla^2 \circ V = k * g \circ (x,y)$ might be approximated at internal mesh points by

$$0 = -k * g \circ (X_{i,j}\, y_{i,j}) + \frac{V_{i+1,j} - 2 * V_{i,j} + V_{i-1,j}}{X^2} + \frac{V_{i,j+1} - 2 * V_{i,j} + V_{i,j-1}}{Y^2}$$

and $V = k * h \circ (s)$ at boundary points (for simplicity we are not considering curved boundaries) would simply become

$$0 = V - k * h \circ \left[x(s),\ y(s)\right]$$

At each of m times n mesh points, there are two associated independent variables (coordinates x and y of the mesh point), and the dependent variable V. For bookkeeping purposes, a control number is also listed at each mesh point. For example, within the region covered by the mesh, there may be boundary points, internal or external points, and changes in the governing equations. Therefore, in general, the difference equations will not be identical at all the mesh points.

Further discussion requires some notational definitions. Often there is more than one dependent variable and necessarily the same number of difference equations at each mesh point. The equations associated with mesh point $P_{i,j}$ are symbolized $f^p{}_{i,j} = 0$. The dependent variables tabulated at $P_{i,j}$ are written $V_{i,j,p}$. The indices i and j refer to the mesh point. The index p lists the equations and corresponding dependent variables at $P_{i,j}$. The independent variables are written as $W_{i,j}$.

The equations at $P_{i,j}$ usually will contain variables listed at $P_{i,j}$ and only a few neighboring points. Therefore, $f^p{}_{i,j} = 0$ is a loosely connected system of equations.

The set of all the $V_{i,j,p}$ and $W_{i,j}$ will be relabeled Z_m and X_r respectively. The homogeneous difference equations may now be written

$$f^p{}_{i,j} \circ (k, Z_m, X_r) = 0$$

to show the functional dependence. Note that each $f^p{}_{i,j}$ usually depends on only a few of the Z_m and X_r. If the numerical values of the Z_m are chosen

properly, they will simultaneously satisfy all the $f^{p}_{i,j} = 0$. This is an exact solution to the system for the parameter value k, and will be written $\bar{Z}_m(k)$. A set of Z_m which is not an exact solution is a trial solution, and will simply be written $Z_m(k)$.

E.3 The Convergence Process

Let a known solution $\bar{Z}_m(k)$ for k = A be tabulated throughout the mesh. The solution for k = B is desired. The range of k is divided into q equal (for simplicity) parts, generating a sequence of q + 1 values of k over the interval A to B. Denote this sequence by k_q. In a time dependent problem the parameter enters naturally as time, so that k = time.

The convergence process uses the solution $\bar{Z}_m(k_q)$ to proceed toward the solution $\bar{Z}_m(k_{q+1})$. Starting with k = A, the process is repeated (as k ⟶ B) so that it converges to the final solution $\bar{Z}_m$, for k = B.

At this time the equation, point, and system residuals (or errors) need to be defined. The equation residual $E^{p}_{i,j}$ for equation $f^{p}_{i,j}(k, Z_m) = 0$ is simply

$$E^{p}_{i,j}(k, Z_m) = f^{p}_{i,j}(k, Z_m)$$

The point residual is the sum of the squares of the equation residuals at the point.

$$R_{i,j}(k, Z_m) = \sum_{p} (E^{p}_{i,j})^2$$

The system residual is the sum of all the point residuals.

$$S(k, Z_m) = \sum_{i,j} R_{i,j}$$

For a given k, the system residual $S(k, Z_m)$ may be interpreted as a surface above an m dimensional hyperplane. A point on the hyperplane represents a possible choice of values of the set of independent mesh

variables Z_m. The height of the surface above a point in the plane is the system residual for the mesh variable configuration represented by that point. A point Z_m, where S = 0 is clearly a solution to the system.

E.4 Algorithm

The algorithm for getting from the solution $\bar{Z}_m(k_n)$ for k_n to the solution $\bar{Z}_m(k_{n+1})$ for k_{n+1} is now described. Since the solution for k_{n-1} is available (except at k_n = A), a likely prediction $\bar{Z}_m(k_{n+1})$ for the solution $\bar{Z}_m(k_{n+1})$ is

$$\bar{Z}_m(k_{n+1}) \equiv Z_m(k_{n+1}) \equiv \frac{Z_m(k_n) - Z_m(k_{n-1})}{k_n - k_{n-1}} * (k_{n+1} - k_n) + Z_m(k_n)$$

Usually the increment in k is uniform so that the prediction is simply

$$\bar{Z}_m(k_{n+1}) \equiv 2\,\bar{Z}_m(k_n) - \bar{Z}_m(k_{n-1})$$

More elaborate predictors may be built using more of the earlier solutions or some other means peculiar to the particular problem.

The prediction generally will be in error to an extent requiring corrections at many mesh points. The corrector process starts by evaluating the derivatives of each point error $R_{i,j}(k_{n+1})$ with respect to the dependent variables $V_{i,j,p}$ tabulated at point $P_{i,j}$. The result is an array of partial derivatives $D_{i,j,p}$

$$D_{i,j,p} = \frac{d\,R_{i,j}}{d\,V_{1,j,p}}$$

The first correction is written $C_{i,j,p}$ and is added to the guess or prediction. The corrected trial solution is then

$$\bar{Z}_m(k_{n+1}) = Z_m(k_{n+1}) + C_{i,j,p}$$

or in other notation

$$\overset{*}{V}_{i,j,p} = V_{i,j,p} + C_{i,j,p}$$

The correction array $C_{i,j,p}$ is given by

$$C_{i,j,p} = -L * \frac{D_{i,j,p} * R_{i,j}(k_{n+1})}{\sum_{p} (D_{i,j,p})^2}$$

where

$$0 < L \leq 1$$

Essentially, the p partials at a point determine a "gradient" direction in which the error changes the fastest. This calculation assumes that the interaction with the surrounding points is less than the influence of the point on its own error.

The correction at each point is made in the negative of the "gradient" direction. The magnitude of the point correction is the point error divided by the rate of change of the point error. Even though the errors at surrounding points are affected as each point is moved, this correction method does indeed converge for many systems.

L is introduced to prevent overshoot and to avoid making the errors bigger, leading to instability. This is important at the start of the correction cycle when the errors are relatively large. In a nonlinear problem, generally L should start around 0.1 and go to 1.0 as the errors diminish. See Figure 1.

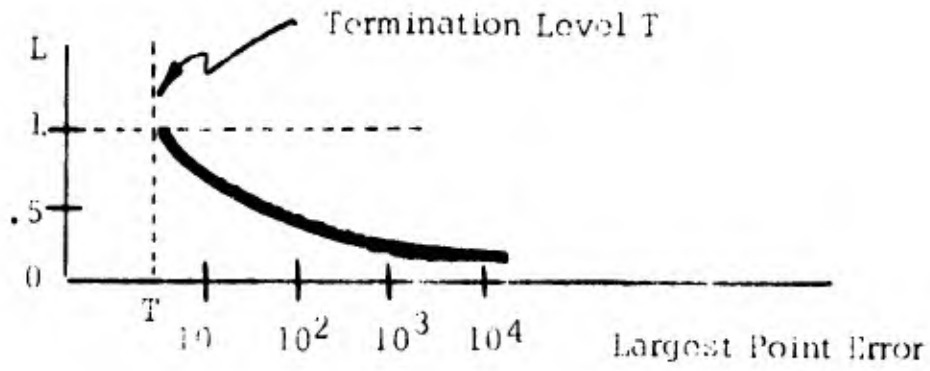

FIGURE 1

The value of L as a function of the largest point residual is determined mostly by experience with a given problem.

A corrector termination level, T, is set so that when the largest point error is less than T, the trial solution is considered sufficiently accurate and the computations for the next value of k are started.

The procedure is repeated until the solution Z_m for k = B is reached.

During the corrector procedure, many artificial devices can be used to vastly speed the convergence in particular problems. A great deal depends on the investigator's ingenuity and his intuitive feel for the behavior of the solution.

E.5 Computational Aspects

In implementing the algorithm on a digital machine, several aspects deserve attention.

The point errors will usually be reduced in some parts of the mesh faster than others, and therefore will reach an acceptable value well before other parts. Much time can be saved if zeros are placed in the correction array wherever the point error is less than the cutoff level. They are called zero points for the moment. Then in the next corrector cycle no calculations are performed at zero points for which the neighbor points they depend on are also zero.

The elimination of calculations at zero points also avoids the round-off noise that soon arises and becomes evident at points requiring little correction.

For simple systems of equations, the derivatives may be evaluated by an analytic formula derived from the difference equations. In more complicated cases, it is usually easier and just as fast to take a finite difference. For one thing, this allows the alteration of the system equations without having to rederive the derivative formulas. We found this convenient in our program for elasto-plastic dynamics where the governing equations are exceedingly complicated.

In many physical problems, especially those in fields, stress analysis, etc., a reasonably good initial prediction can be made. For

example, Frocht's method of "Linear Rosettes" in linear static stress analysis is a fast computation and can provide a good start for a nonlinear system.

E.6 Convergence Theory

For simplicity, consider a one-dimensional mesh in which the point residual involves only the point and its two neighbors. The argument is easily generalized. The point residual at mesh point P_i is R_i and the dependent variable is U_i. The solution for $k = k_n$ is $\overline{Z}_m(k_n)$. Start with $\overline{Z}_m(k_n)$ as an approximation to the solution $\overline{Z}_m(k_{n+1})$. The assumed continuity of Z_m with respect to k implies that for sufficiently small $\Delta k = k_{n+1} - k_n$ the largest point error can be held to any desired level.

The correction to be applied at each point P_i is

$$C_i = \frac{-L * R_i}{\frac{dR_i}{dU_i}}$$

The change in the residual at point P_i for infinitesimal L is

$$\Delta R_i = C_{i-1} * \frac{dR_i}{dU_{i-1}} + C_i * \frac{dR_i}{dU_i} + C_{i+1} * \frac{dR_i}{dU_{i+1}}$$

$$\frac{\Delta R_i}{\Delta L} = -\left[R_{i-1} \frac{\frac{dR_i}{dU_{i-1}}}{\frac{dR_{i-1}}{dU_{i-1}}} + R_i + R_{i+1} \frac{\frac{dR_i}{dU_{i+1}}}{\frac{dR_{i+1}}{dU_{i+1}}} \right]$$

Clearly $\Delta R_i/\Delta L$ should be much less than zero for rapid convergence.

In general, $\Delta R_i/\Delta L$ can be written as a well behaved function of several variables. It is hoped that in the region of interest $\Delta R_i/\Delta L \ll 0$. For a particular set of equations, the determination of the region where $\Delta R_i/\Delta L$ is negative may be very complicated. Usually physical intuition

is sufficient to assess the probable convergence or divergence of the method. The iterations will probably converge if the equations are such that the point residual depends more strongly on the variables at that point than it does on the variables at the neighbor points. If a given system is of the variable space, etc.) can be used to investigate the regions where $\Delta R_i/\Delta L$ is negative.

APPENDIX F: REFERENCES

1. Eringen, A. Cemal, "Nonlinear Theory of Continuous Media," McGraw-Hill Book Company, Inc., New York (1962).

2. Sokolnikoff, I. S., "Tensor Analysis," New York (1951).

3. Sokolnikoff, I. S., "Mathematical Theory of Elasticity," McGraw-Hill Book Company, Inc., New York (1956).

4. Houwink, R., "Elasticity, Plasticity and Structure of Matter," Dover Publications, Inc., New York (1958).

5. Lichnerowicz, A., "Elements of Tensor Calculus," John Wiley & Sons, Inc., New York (1963).

6. Wrede, Robert C., "Vector and Tensor Analysis," John Wiley & Sons, Inc., New York (1963).

7. Hodgman, Charles D., "Handbook of Chemistry and Physics," Chemical Rubber Publishing Co., Cleveland, Ohio (1940).

8. Riney, T. D., "Theoretical Hypervelocity Impact Calculations Using the Picwick Code," Air Proving Ground Center, Eglin Air Force Base, Florida (1963).

9. Wylie, C. R. Jr., "Advanced Engineering Mathematics," McGraw-Hill, Book Company, Inc., New York (1960).

10. Ralston, Anthony and Herbert S. Wilf, "Mathematical Methods for Digital Computers," John Wiley & Sons, Inc., New York (1962).

11. Coulson, C. A., "Waves," Interscience Publishers, Inc., New York (1962).

12. Thomas, Tracy Y., "Plastic Flow and Fracture in Solids," Academic Press, New York (1961).

13. Grinter, L. E., "Numerical Methods of Analysis in Engineering," MacMillan Company, New York (1949).

14. Hildebrand, F. B., "Introduction to Numerical Analysis," McGraw-Hill Book Company, Inc. (1956).

15. Webster, A. G., "Partial Differential Equations of Mathematical Physics," Dover Publications, Inc. (1955).

16. Thomas, Tracy Y., "Tensor Analysis and Differential Geometry," Academic Press, New York (1961).

17. Lapidus, Leon, "Digital Computation for Chemical Engineers," McGraw-Hill Book Company, Inc., New York (1962).

18. Freudenstein, Ferdinand and Bernard Roth, "Numerical Solution of Systems of Nonlinear Equations," Journal of the Association for Computing Machinery, Assoc. for Computing Machinery, (1963).

19. Brode, H. L. and R. L. Bjork, "Cratering From a Megaton Surface Burst," Proceedings of the Geophysical Laboratory, Lawrence Radiation Laboratory Cratering Symposium, Livermore, Calif. (1961).

20. Rajnak, S. and F. Hauser, "Plastic Wave Propagation in Rods," Symposium on Dynamic Behavior of Materials, ASTM Special Technical Publication No. 336, American Soc. for Testing and Materials, Philadelphia, Pa. (1962).

21. Harlow, Francis H., "Two-Dimensional Hydrodynamic Calculations," Los Alamos Scientific Laboratory, Mex. (1959).

22. Wilkins, Mark L. and Richard Giroux, "The Calculation of Stress Waves in Solids," Proceedings of the Sixth Symposium on Hypervelocity Impact (1963).

23. Kolsky, H., "Stress Waves in Solids," Dover Publications, Inc., New York (1963).

24. Daly, Bart J., "The Bounding of Instabilities of the PIC Difference Equations, Los Alamos Scientific Laboratory, Mex. (1962).

BLANK PAGE

Unclassified

Security Classification

DOCUMENT CONTROL DATA - R&D

(Security classification of title, body of abstract and indexing annotation must be entered when the overall report is classified)

1. ORIGINATING ACTIVITY *(Corporate author)*

Utah Research & Development Co., Inc.
Salt Lake City, Utah

2a. REPORT SECURITY CLASSIFICATION

Unclassified

2b GROUP

3. REPORT TITLE

THEORETICAL AND EXPERIMENTAL STUDY OF LOW-VELOCITY PENETRATION PHENOMENA

4. DESCRIPTIVE NOTES *(Type of report and inclusive dates)*

Final Report Phases I & II, 25 June 1963-24 June 1964

5. AUTHOR(S) *(Last name, first name, initial)*

Cannon, Emerson T., Dr.

6. REPORT DATE	7a. TOTAL NO. OF PAGES	7b. NO. OF REFS
28 June 1964	103	24

8a. CONTRACT OR GRANT NO.

DA19-129-AMC-150(X) (O.I: 9114)

b. PROJECT NO.

ARPA Order No. 267 Amendment 4

c.

d.

9a. ORIGINATOR'S REPORT NUMBER(S)

9b. OTHER REPORT NO(S) *(Any other numbers that may be assigned this report)*

10. AVAILABILITY/LIMITATION NOTICES

Distribution is unlimited.
Release to CFSTI is authorized.

11. SUPPLEMENTARY NOTES

12. SPONSORING MILITARY ACTIVITY

U. S. Army Natick Laboratories
Natick, Massachusetts

13. ABSTRACT

This report is a technical summary of Phases I and II of a theoretical and experimental study of low-velocity penetration phenomena.

Phase I has consisted of a literature survey to determine the state of the art. The results are summarized and a bibliography is included. It is concluded that semi-empirical correlation formulae and over-simplified theories do not give the results needed for armor design and are inadequate as a guide to understanding low-velocity impact phenomena.

Phase II has consisted of the development of a new method of describing the elasto-plastic behavior of a material under impact conditions. The non-linear differential equations involved are expressed in a tensor formulation particularly suitable for computer calculations. The method used is very general and allows a wide variety of boundary conditions and material properties to be used. The work is described and the results of preliminary calculations are presented in this report.

DD FORM 1 JAN 64 1473

Unclassified

Security Classification

14. KEY WORDS	LINK A		LINK B		LINK C	
	ROLE	WT	ROLE	WT	ROLE	WT
Penetration	8		9			
Low-velocity	0		0			
Impact	8		9			
Armor	4		4			
Correlation techniques			8			
Mathematical models			8			
Viscoelastic materials	9		9			

INSTRUCTIONS

1. **ORIGINATING ACTIVITY:** Enter the name and address of the contractor, subcontractor, grantee, Department of Defense activity or other organization *(corporate author)* issuing the report.

2*a*. **REPORT SECURITY CLASSIFICATION:** Enter the overall security classification of the report. Indicate whether "Restricted Data" is included. Marking is to be in accordance with appropriate security regulations.

2*b*. **GROUP:** Automatic downgrading is specified in DoD Directive 5200.10 and Armed Forces Industrial Manual. Enter the group number. Also, when applicable, show that optional markings have been used for Group 3 and Group 4 as authorized.

3. **REPORT TITLE:** Enter the complete report title in all capital letters. Titles in all cases should be unclassified. If a meaningful title cannot be selected without classification, show title classification in all capitals in parenthesis immediately following the title.

4. **DESCRIPTIVE NOTES:** If appropriate, enter the type of report, e.g., interim, progress, summary, annual, or final. Give the inclusive dates when a specific reporting period is covered.

5. **AUTHOR(S):** Enter the name(s) of author(s) as shown on or in the report. Enter last name, first name, middle initial. If military, show rank and branch of service. The name of the principal author is an absolute minimum requirement.

6. **REPORT DATE:** Enter the date of the report as day, month, year; or month, year. If more than one date appears on the report, use date of publication.

7*a*. **TOTAL NUMBER OF PAGES:** The total page count should follow normal pagination procedures, i.e., enter the number of pages containing information.

7*b*. **NUMBER OF REFERENCES:** Enter the total number of references cited in the report.

8*a*. **CONTRACT OR GRANT NUMBER:** If appropriate, enter the applicable number of the contract or grant under which the report was written.

8*b*, 8*c*, & 8*d*. **PROJECT NUMBER:** Enter the appropriate military department identification, such as project number, subproject number, system numbers, task number, etc.

9*a*. **ORIGINATOR'S REPORT NUMBER(S):** Enter the official report number by which the document will be identified and controlled by the originating activity. This number must be unique to this report.

9*b*. **OTHER REPORT NUMBER(S):** If the report has been assigned any other report numbers *(either by the originator or by the sponsor)*, also enter this number(s).

10. **AVAILABILITY/LIMITATION NOTICES:** Enter any limitations on further dissemination of the report, other than those imposed by security classification, using standard statements such as:

(1) "Qualified requesters may obtain copies of this report from DDC."

(2) "Foreign announcement and dissemination of this report by DDC is not authorized."

(3) "U. S. Government agencies may obtain copies of this report directly from DDC. Other qualified DDC users shall request through _____."

(4) "U. S. military agencies may obtain copies of this report directly from DDC. Other qualified users shall request through _____."

(5) "All distribution of this report is controlled. Qualified DDC users shall request through _____."

If the report has been furnished to the Office of Technical Services, Department of Commerce, for sale to the public, indicate this fact and enter the price, if known.

11. **SUPPLEMENTARY NOTES:** Use for additional explanatory notes.

12. **SPONSORING MILITARY ACTIVITY:** Enter the name of the departmental project office or laboratory sponsoring *(paying for)* the research and development. Include address.

13. **ABSTRACT:** Enter an abstract giving a brief and factual summary of the document indicative of the report, even though it may also appear elsewhere in the body of the technical report. If additional space is required, a continuation sheet shall be attached.

It is highly desirable that the abstract of classified reports be unclassified. Each paragraph of the abstract shall end with an indication of the military security classification of the information in the paragraph, represented as *(TS)*, *(S)*, *(C)*, *or (U)*.

There is no limitation on the length of the abstract. However, the suggested length is from 150 to 225 words.

14. **KEY WORDS:** Key words are technically meaningful terms or short phrases that characterize a report and may be used as index entries for cataloging the report. Key words must be selected so that no security classification is required. Identifiers, such as equipment model designation, trade name, military project code name, geographic location, may be used as key words but will be followed by an indication of technical context. The assignment of links, rules, and weights is optional.